International Journal of Environmental Science and Technology (2023) 20:1053–1080
https://doi.org/10.1007/s13762-022-03965-8

REVIEW

Current trends on extraction of water from air: an alternative solution to water supply

M. A. Siddiqui[1] · M. Anique Azam[1] · M. Munim Khan[1] · S. Iqbal[1] · M. Usman Khan[1] · Y. Raffat[1]

Received: 7 December 2021 / Revised: 11 January 2022 / Accepted: 14 January 2022 / Published online: 4 February 2022

Abstract

The world has been finding new ways for harvesting water that can fulfill our daily needs among which atmospheric water generation (AWG) is an emerging solution, currently under continuous development process. By this process, ambient humidity in the air can be extracted mechanically via cooling and interception, or chemically via absorption, for use as needed. This study reviews various technologies of AWG that are being used for harvesting water using the atmospheric air, with their comparison based on outputs, efficiencies, and economics. Materials including new hydrogel formations which can be used for the advancement of the technology are reported. Peltier-thermoelectric cooler-based AWG and desiccant-based AWG have been thoroughly discussed throughout the review. The study reflects the importance of harvesting water from the air as this technology has the potential to attain self-sustainability without relying on a freshwater source, both actively and passively.

Keywords Air-water generator · SDG 6 · Absorption cycle · Vapor compression cycle · Thermoelectric cooling · Desiccants · Solar energy

Abbreviations

A	Wet surface area of $LiAlO_2$ (m^2/g)
A_1	Top surface area
A_2	Horizontally projected area of the solar still (m^2)
AWG	Air-water generator
AC	Activated carbon
ACF	Active carbon fiber
BLDC	Brushless DC motor
CNT	Carbon nanotubes
COP	Coefficient of performance
DRH	Deliquescent relative humidity
DC	Direct current
DS-HCBSS	Double slope half cylinder basin solar still
EPNS	Engineered-photothermal nano-composite sheet
E_L	Elevation above the sea level (m)
e	Actual vapor pressure
FC	Fuel cell
H	Total radiation incident (W/m^2)
h_{fg}	Latent heat of water (J/Kg)
I	Solar Intensity (W/m^2)
K_m	Thermal conductivity (W/m.K)
$LiAlO_2$	Lithium aluminate
LTPEMFC	Low-temperature proton exchange membrane fuel cell
MC	Microbial cell
MCFC	Molten carbonate fuel cell
MDC	Microbial desalination cell
MEC	Microbial electrolysis cell
MFC	Microbial fuel cell
MRC	Microbial reverse electro dialysis cell
MOF	Metal–organic framework
m_i	Mass of NBHA after adsorption
m_a	Initial mass of NBHA before adsorption
PAM	Polyacrylamide
S_m	Seebeck coefficient
PV	Photovoltaic
PWM	Pulse width modulation
P_{TEC}	Thermo-electric power consumption
P_{Sta}	Station pressure (milli-Bar)
P_w	Saturation pressure of water vapor at 25 °C
P_a	Atmospheric pressure
Q_H	Amount of heat dissipated

Editorial responsibility: Maryam Shabani.

✉ M. A. Siddiqui
mubashir@neduet.edu.pk

[1] Mechanical Engineering Department, NED University of Engineering and Technology, Karachi 75270, Sindh, Pakistan

Q_{ad}	Amount of adsorbed water (mol-H_2O/mol-$LiAlO_2$)
Q_v	Useful heat
q_e	Rate of heat transferred via radiation (W/m^2)
RH	Relative humidity (%)
R_m	Electrical resistance
SiO_2	Silica gel
T	Ambient temperature (°C)
T_p	Time period of light irradiation
TEC	Thermo-electric couples
T_H	Hot side temperature (°C)
T_d	Dew point temperature (°C)
TSS	Tubular solar still
UV	Ultra-violet
VCC	Vapor compression cycle
$\overline{\omega}_{month}$	Mean humidity ratio (kg_{water}/kg_{air})

Introduction

The humans living on earth are dependent on freshwater availability which, unfortunately, is not readily available due to major portion of it being saline in nature. The share of saline water is 97.5% and the rest 2.5% is drinkable. Glaciers and icecaps hold approximately 70% of the world's water and the remaining percentage of water is in lakes that are underground. Lakes (around 67%), soils (around 12%), swamps (around 9%), rivers (around 2%), and water vapor make up the useable water (around 9%) and there is also a very small fraction of water in humans (0.8%)(Gleick 1993; WEO 2016; Oki and Kanae 2006). The decrement and scarcity of usable and safe water resources for human usage is a global issue that is rising since it is an essential resource for living beings (Mendoza-Escamilla et al. 2019). A major problem adding to the scarcity is the rapid depletion of underground water resources which are being used by many countries uncontrollably (Shweta and Nerlekar 2017). Arid and semi-arid nations suffer from deficits in their stock of drinkable water (Khalil et al. 2016). Jury and Vaux (2007) reinstated that the United Nations predicted a severe shortage of water for 48 countries by 2025. Among different techniques like membrane filtration, ion exchange, advanced oxidation technology, etc. for the access of clean drinking water, atmospheric water harvesting may be a viable option as suggested by NRC (1999). Baysens and Milimouk (2000) identified the resources of alternative water on earth. Atmospheric water can be found in three different forms: clouds in the sky, fog at the surface of the land, and vapor present in the air. El-Hasan (2017) found that the water obtained from the atmosphere was clean and it met the drinking requirement under nominal air purity. The atmosphere comprises of water vapor of which 35% is wasted that can be utilized for harvesting water. A device that converts moisture from the air into drinkable, sterile water for consumption is known as an atmospheric water generator, abbreviated as AWGs (Tripathi et al. 2016). Many dehumidification methods can be used to collect water from the atmosphere such as utilization of the Peltier principle, vapor compression cycle, desiccants, etc. The air–water generators usually work on the vapor compression cycle. The AWG has the ability and potential to make prospective researchers go into new horizons of getting drinking water from a machine in a way that is solar assisted and energy efficient (Inbar et al. 2020; Tu et al. 2018). Sami (2020) investigated solar energy which is considered a renewable, pollution, and noise-free source, for utilization with the Peltier combination in air-water generators. Solar energy can be used via PV cells or sorption-based processes for harvesting moisture from the air. It can also help to supply water in emergency response (Kim et al. 2018). Research on nanomaterials have been advancing recently and new nanomaterials designed and added to the literature. Xing et al (2017) showed designed bioinspired nanocomposite bearing capability of water purification requirements such as waste water treatment and dye removal. Such materials are not only ecofriendly to produce but can also be used in large-scale applications. Guo et al. (2018) added enhanced adsorption for 2D carbon nanomaterials which proved promising for adsorption-based AWG. Hydrogels, on the other hand, found their applications in water treatment best-practices (Jiao et al. 2015). While harvesting water from air as a macro-molecule might be intuitive, smart nanomaterials were also designed by Xu et al. (2021) for electrocatalysis in water splitting evolving hydrogen, which may be recombined to yield significant purity of produced water. El-Dessouky and Ettouney (2002) also reported that it takes 2000–5000 L of water to produce one person's daily food, which brings the issue of water scarcity into even sharper focus. The freshwater availability is very important for the economic development of people living in remote areas especially if they are deprived of the annual rainfall while also lacking sufficient lakes and rivers to meet the needs of the locals (Oliver and De-Rautenbach 2002; Abdul-Wahab 2008; He et al. 2020).

What is atmospheric water generator?

Basics of AWG

Nitrogen, oxygen, and water vapor combine to form majority of the air around us. An AWG is an apparatus that utilizes dehumidification via condensation technology for extracting

water vapor from air. After that, water is filtered and treated by passing it through a series of channels that include carbon, reverse osmosis, and UV sterilization lights. As a consequence, purified drinking water is collected from the atmosphere (Tripathi et al. 2016).

The use of AWG for water production must fulfill the three requirements before it can be used for its desired purpose as laid down by WHO discussed in Dash et al. (2015).

1. Potability of water—The water generated through the AWG must meet the quality standards of drinking given by WHO.
2. Simple design—The design of the AWG should be such that it can be operated with limited technical expertize.
3. Security and wellbeing—The AWG configuration should not be a danger and risk to any person during its standard functioning.

Technologies of AWG

An AWG is a moisture extracting system from humid air utilizing different technologies. The methods used by the water generator to collect atmospheric water are through condensing the air by cooling it beneath its dew point, or dehumidifying the air by exposing it to a desiccant, where the former is termed active and the latter as passive (Kord 2019).

An active AWG, also known as the conventional AWG, requires an external source of energy (electricity) to stimulate the condensation process. Usually a system comprising of a compressor, heat exchangers/humidity condenser, and a fan, is required to make air saturated by cooling it below the psychrometric dew point temperature (Kord 2019).

Passive AWG does not require any electrical power supply to produce water out of the humid ambient air. It does not require power-consuming components, usually compressors (Kord 2019). The passive AWG employs the wet-dry desiccant technique that works on the principle of an absorption–desorption cycle.

Cooling condensation type (active AWG)

Prominent methods

An active AWG employs two technologies for dehumidifying the air, one that works on the principle of a Vapor Compression cycle (where electrical energy is first converted to shaft work and then thermal energies) whereas the other uses a thermoelectrical cooler using a Peltier effect (where electrical energy is directly converted to a temperature gradient) discussed by Dash et al. (2015). Both the technologies are discussed in subsequent sections.

Vapor compression cycle

It consists of moving components including, but not limited to, a refrigerant-side evaporator, compressor, and a refrigerant-side condenser, to cool the air and extract water from the air. The cooling condensation type AWG works on a vapor compression cycle. In this method, the airstream circulates around the evaporator's cooling coil so that the water in the air reaches its saturation point as illustrated in Fig. 1 reproduced from Dash et al. (2015)

A liquid refrigerant is moved throughout the vapor compression refrigeration system which serves as the carrier that withdraws heat from the conditioned space before rejecting it to the atmosphere. A typical vapor compression cycle is comprised of four components which are illustrated in Fig. 2. The role of the compressor is to compress the refrigerant which enters as saturated or superheated vapor (Rao 2003). This compression results in high pressure and temperature of the refrigerant. The compressed vapor then condenses and reaches condensing temperature and pressure. After that, it passes through the expansion device where the pressure goes down suddenly undergoing flash evaporation. The Joule–Thomson effect reduces liquid refrigerant and vapor mixture temperature (Perry et al. 2000). This mixture is then sent to the evaporator where it exchanges heat with the hot air, making the air cooler and the refrigerant then enters the compressor as saturated vapor to complete the cycle.

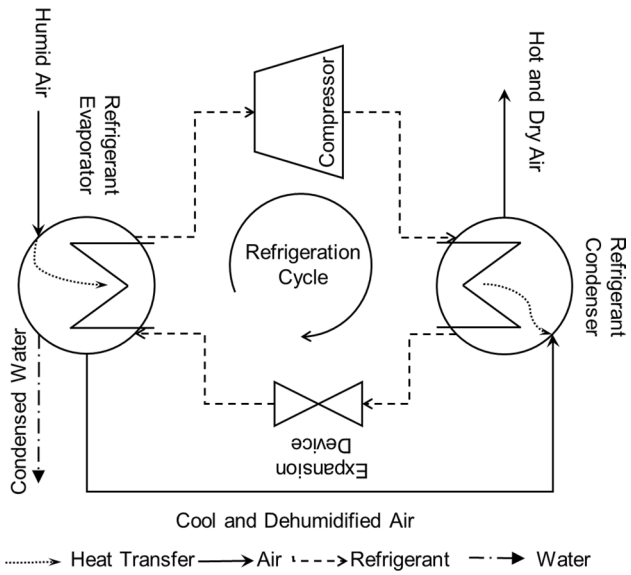

Fig. 1 Schematic of vapor compression cycle for atmospheric water generation

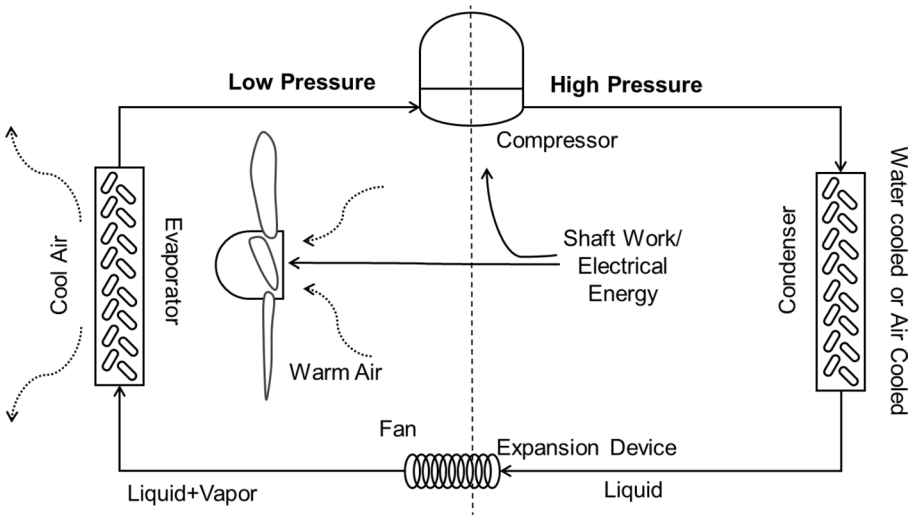

Fig. 2 Standard single stage vapor compression cycle

Primitive thermoelectric (Peltier) coolers

The Peltier Effect Thermoelectric Cooling Technology is similar to Vapor Compression Refrigeration Technology, in a sense that a Peltier device is used to reach the desired saturation point temperature without mechanical work or moving components. Peltier devices are small, have lesser to no moving parts, are energy efficient, and last longer with little maintenance (Dash et al. 2015). Two heat exchange surfaces form a traditional TEC device. If the direct current is permitted to pass through the device, the heat is transferred, producing a cooler and a hotter end (He et al. 2019). Varying temperature and humidity have a huge influence on the vapor content in air. The warmer air is able to retain large quantities of water vapor and vice versa. The Peltier device consists of a hot and a cold side and its working is entirely dependent on the air passing through these hot and cold sides. The air is initially passed over the cold side, where it cools and its capacity to store moisture decreases, resulting in moisture condensation. In Ramya and Roopa (2020), for running of the Peltier cooler without any damage, this air then moves through the hot side to cool it. The water that is obtained via condensation is collected into the tank or any kind of clean reservoir and then passed through filters for further purification. In Fig. 3 the block diagram of the AWG device using Peltier is shown from Suryaningsih and Nurhilal (2016). The features of the Peltier device discussed by Rakesh et al. (2016) are listed as follows:

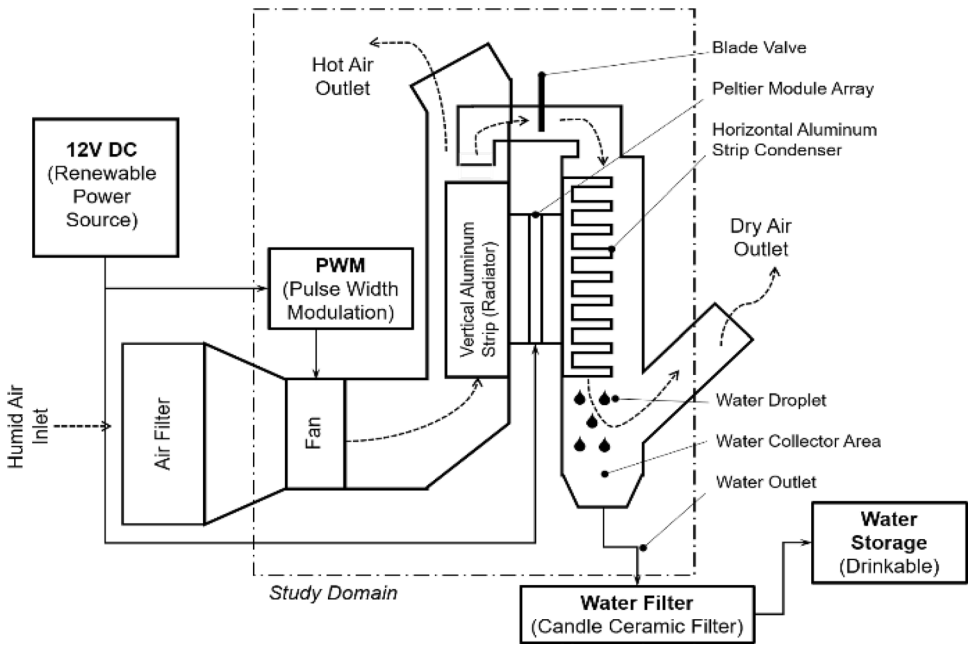

Fig. 3 Basic schematic of Peltier AWG from Suryaningsih and Nurhilal (2016)

1. The Peltier cooler has no moving parts, hence the need for maintenance is relatively less.
2. There is no Utilization of Chloro-Fluoro Carbons (refrigerant and emissive gases) which harm the ozone layer of the earth.
3. It requires relatively less current as compared to the conventional AWGs.
4. It has a flexible shape and small size.
5. It have an efficiency rather a coefficient of performance, and hence would always use a fraction of provided electrical energy to condense water vapor.

Novel models on thermoelectrically cooled AWGs

Proceedings in the literature

Many researchers have drawn their attention toward the working of a Peltier-based technology because of its versatility and design flexibility. Researchers have developed a number of models, both experimental and numerical, to determine the volume and rate of water produced by the thermo-electric cooling-based AWG while incorporating new concepts into the technology. Considering the benefits offered by the Peltier device mentioned in the preceding section, a portable Peltier-based AWG was fabricated due to its simpler design, endurance capability, and capacity. The device was constructed in India and the water generated was then segregated and filtered by using a microcontroller. The water output in Sanjana et al. (2019) was found to be one liter of water every hour during the day.

Kumar et al. (n.d.) discussed the working of any AWG under the cooling condensation types. The evaporator, compressor, and condenser are the three main components of a traditional cooling system and a TEC has some analogous components as well. When electrons go from a minimal energy level in a *p*-type semiconductor to a greater energy level in an *n*-type semiconductor, they ingest energy as heat. The energy necessary for those electrons to pass through the gadget is provided by the electrical power. Energy is ejected to a heat sink at the hot junction when electrons migrate from a greater energy level (*n*-type) to a minimal energy level (*p*-type).

To ensure better performance of Peltier-based AWG, simulations were run on the thermo-electric cooling type AWG utilizing the CFD Software. CFD was used to study the heat exchange between in-contact solids and ambient air conditions by running the AWG under different amperes of current (1–3 A). By utilizing CFD, the flow of hot air in the surroundings of the AWGs was also calculated. It was revealed that air in this case behaved as an incompressible fluid and it would never flow into a heat sink that also has the heated air going out of it (Lee 2010).

In a new approach that was suggested and validated, the effect of the Peltier coefficient in thermoelectric cooling was also discussed. It was suggested that when calculating the energy balance, a new component called the "seebeck" component be included, which provided the value of the Peltier coefficient with 5% accuracy (Garrido and Casanovas 2014).

The thermodynamic inspection was also carried out on Peltier-based AWG employing 10 thermoelectric coolers as well as heat sinks to boost the rate of heat transmission (Fig. 4). Solar panels were used for the provision of required power to thermoelectric coolers and fan. Findings indicated that escalated temperature of the moving air through the cold path of the thermoelectric coolers increased the water yield and the COP of the system but decreased the optimum airflow rate through the channel. The maximum output of 29.9 mL/h was recorded at 318 K at RH of 75%. The annual performance of the fabricated AWG was also investigated in different cities and the water output was recorded to be the maximum in the city having a high value of relative humidity than the others. The annual water output, electricity use, and system effectiveness are shown in Fig. 5 (Tajeddini et al. 2018). The four main properties of each thermoelectrical cooler are $I_{\max}$, $V_{\max}$, $T_{\max}$ and $Q_{\max}$. The necessary modeling parameters and a hot end temperature in a TEC are defined for the thermoelectric cooler (T_h).

$$S_m = V_{\max}/T_{\max} \tag{1}$$

$$R_m = \left(T_h - \Delta T_{\max}\right) V_{\max}/T_h \times I_{\max} \tag{2}$$

$$K_m = \left(T_h - \Delta T_{\max}\right) V_{\max} I_{\max}/2T_h \Delta T_{\max} \tag{3}$$

The thermo-electric cooler COP is given as:

$$\mathrm{COP} = Q_c/P_{\mathrm{TEC}} \tag{4}$$

To normalize the use of an AWG in rural areas, a design was proposed on the active AWG, based on a thermoelectric cooler, and a prototype was fabricated and tested which ran on solar energy. The prototype was able to meet the minimal WHO drinking water consumption criterion of 2.5 L per

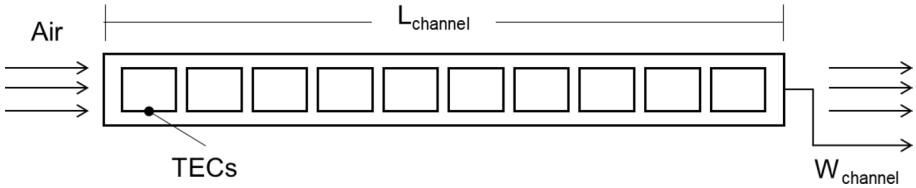

Fig. 4 Layout of thermo-electric coolers and air passaged over them in Tajeddini et al. (2018)

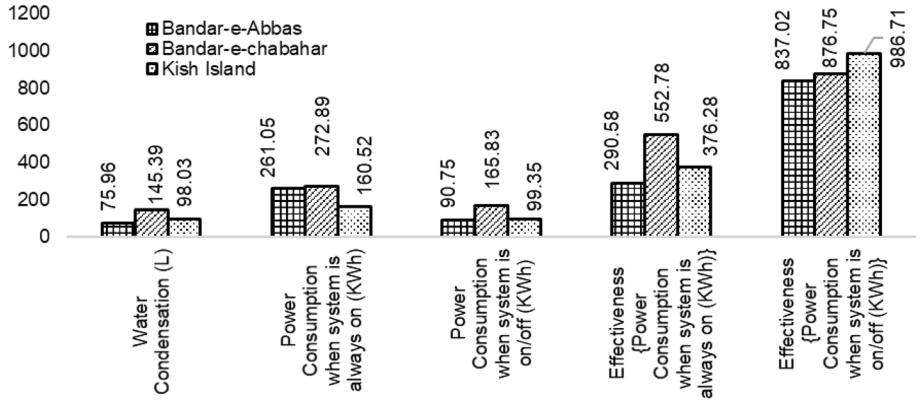

Fig. 5 Annual performance of the fabricated AWG at three different locations (Tajeddini et al. 2018)

capita per day by utilizing 125 W of power, which could easily be generated using a Solar PV panel. The AWG prototype's output was tested with various combinations of Peltier modules, and the water output was recorded, as displayed in Table 1. Water vapor is present in the air, and the vapor content per unit volume is shown in Eq. (5). (Suryaningsih and Nurhilal 2016)

$$\%\text{age} = (0.622e/P_{\text{sta}} - e) \times 100 \tag{5}$$

For P_{sta} (Station Pressure), e and $T_{\max}$ is given by

$$P_{\text{sta}} = 10132.5 \times [(293 - 0.0065EL)/293]5.26 \tag{6}$$

$$e = 0.6108 \times \exp[17.27Td/(Td + 237.3)] \tag{7}$$

$$T_d = 237.3\left[\frac{\ln(RH/100)}{17.27} + \frac{T}{237.3+T}\right]\left[1 - \left[\frac{\ln(RH/100)}{17.27} + \frac{T}{237.3+T}\right]\right]^{-1} \tag{8}$$

Comparison of various AWG technologies with thermoelectric technology

There are various techniques including vapor compression cycle, liquid desiccant, and the use of composite desiccants that can be employed for capturing the moisture from air. In comparison with the Peltier technology, Nørskov et al. (2002) revealed that although the efficiency of the Peltier device is low but it can be increased with the use of the appropriate design.

Two AWGs with thermoelectric cooling technologies were compared in a study. Models A and B (the reference model) were put to the same test. The only change between the two models was that the cold side was covered with a hydrophobic material (Nano-SiO_2 gel). On the hot end, a suction fan was fitted for the air moving across the hot end fins. To help with heat transfer, the TEC's hot-end received cooled air. Use of hydrophobic materials was critical since it aided in boosting the rate at which moist air condensed. The comparison was extremely beneficial because it revealed that model A outperformed model B even in low-humidity environments. The humidity and airflow rate improved the temperature (cold/hot) and water output of prototype A. The operating circumstances in the study that were used to compare the two models are listed in Table 2 (He et al. 2019).

Table 1 Water yield of the fabricated AWG under different TEC modules (Suryaningsih and Nurhilal 2016)

TEC used	Power (W)	Freq (Hz) PWM BLDC	CFM	Air flow rate (m^3/h)	T (°C)	RH (%)	Water yield (L/h)
2	65.52	800	76	129.12	25.3	60	0.028
2	65.52	1200	114	193.69	26	61	0.050
2	65.52	1600	150	254.85	25.5	63	0.100
2	65.52	2000	190	322.81	25.8	58	0.200
4	125.5	800	76	129.12	26	60	0.320
4	125.5	1200	114	193.69	26	59	0.410
4	125.5	1600	150	254.85	26.5	61	0.490
4	125.5	2000	190	322.81	27	62	0.610

Another comparison was performed by Bradshaw (2016) between two prototypes based on thermoelectric cooling using condensing surfaces of aluminum and copper respectively. Aluminum was found to perform better, producing condensate of 5.9 mL on average. The results also suggested that thermal conductivity (of Aluminum and Copper) was not an important parameter for assessing the performance of the device.

A comparison of the Peltier and cooling condensation was also made by Pontious et al. (2016) by designing two prototypes, one working on the Peltier-based concept and the other one on the heat exchanger-based concept. The heat exchanger-based AWG works on the principle that air is allowed to pass through a chamber that employs a heat exchanger powered by a fan that runs on solar energy. As the warm air is passed through the chiller (heat exchanger), the condensation of water vapor takes place. It was revealed that the AWG device using the Peltier-based concept was able to produce 10.2 mL of water whereas the device using the concept of the heat exchanger was able to produce 82.4 mL water, which was 8 times higher. The Peltier device consumed less power and was less expensive as compared to the heat exchanger-based device.

Solar-powered active AWGs

Solar-powered vapor compression cycle for water generation

The energy from the sun is the most readily available and ample source of energy. The use of solar-powered AWG comes into play where the necessary electricity can be produced using solar panels and, when the amount of electricity available for daily consumption is not enough. The main issue is the lack of knowledge on the performance characteristics of a solar-powered AWG. To address this knowledge gap, a simulation model was developed by Aye et al. (2013) focusing on the individual phenomenon including availability of the solar radiation, PV power output, battery storage, amount of moisture in air, and mass and heat transmission at the vapor compression refrigeration in the experiment. The simulations were run on hourly basis for the whole year. The AWG's monthly average daily efficiency was found out using Eq. (9).

$$\eta_{\text{avg}} = \left[\sum_{d=1}^{n} m_{\text{water},d}\right] \Big/ \left[\left(\sum_{d=1}^{n} m_{\text{air},d}\right)\overline{\omega}_{\text{month}}\right] \tag{9}$$

The monthly average daily water yield, efficiency of the device and the CCOP are given in Table 3. The efficiency of the water device was found and it was between 5.4 and 9.3%. An air–water generator system with a sufficiently big current output drive was created by Kumar and Sukumar (2019) using solar technologies consisting of cooling components, air circulators and solar panel. In situations of water shortage, this method has been shown to be useful (Fig. 6).

Sami (2020) designed a numerical model with various components, including solar insolation, air humidity, atmospheric temperature and rate of air flow to examine the performance of the solar-powered atmosphere water generator. Solar radiation, atmospheric air temperature and relative humidity were found to have significant effect on the output. It was also shown that airflow parameters like relative humidity and surrounding atmospheric temperature significantly affected power of compressor. A new AWG system by Salek et al. (2018), comprising of three parts illustrated in Fig. 7 was suggested to increase the quantity of water produced with reduced power usage. The system generated water from two channels, humid air and salty water, and AWG's water output increased by 35%. A mobile solar PV air-water generator including a water-producing unit

Table 2 Operating conditions in He et al. (2019)

Scenarios	1	2	3	4	5	6
Airflow rate (m^3/h)	30	30	30	30	50	70
RH (%)	60	70	80	90	60	60

Table 3 Monthly average daily water yield, system efficiency and compressor CCOP (Aye et al. 2013)

Performance specifications	Water yield	Efficiency (%)	COP	Performance specifications	Water yield	Efficiency (%)	COP
1	22.4	7.4	4.3	7	36.4	9.3	4.9
2	23.7	7.6	4.4	8	36.6	9.3	4.9
3	27.4	7.7	4.4	9	32.6	8.7	4.6
4	28.9	7.8	4.4	10	30.3	8.0	4.5
5	28.0	7.5	4.3	11	23.5	7.3	4.3
6	36.2	8.8	4.7	12	15.3	5.4	4.1

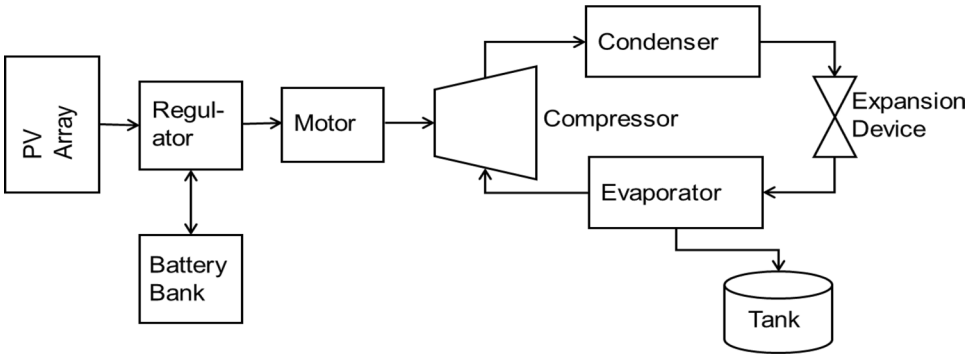

Fig. 6 Schematic diagram of a solar driven AWG by Aye et al. (2013)

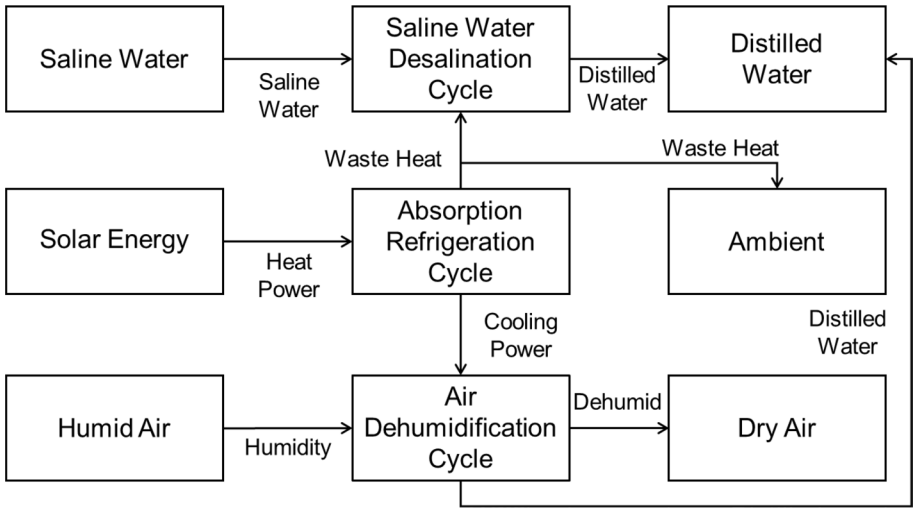

Fig. 7 Block diagram of the new AWG in Salek et al. (2018)

was built and tested effectively by Runze et al. (2020). The device might be a lifeline for anyone in trouble in tropical waters, not just by providing drinking water but also by aiding in their rescue. The device's main flaw was its poor condensation efficiency, which was caused by the higher airflow velocity and inadequate compressor cooling.

Solar-powered thermoelectric cooler for water generation

Solar energy was also utilized in powering the active AWG in place of grid electricity. The utilization of solar energy in driving water condensation system (active AWG) was found to have a great economic benefit which was due to the free availability of the power source and less maintenance requirement (Lee 2010; Kadhim et al. 2020). Various prototypes in the literature were tested using solar energy, and one such prototype testing was carried out by Huajun and Chengyin (2010) in Thailand. It revealed that utilizing solar energy as the power source for water production might result in saving lives of multiple persons by generating ample water and was also very economic as compared to the AWG utilizing grid generated electricity.

The installation and experimental test of a drinking water collection device based on solar energy was conducted by attaching a single thermoelectric framework to multiple extended surfaces for calculating the water production rate. The cold side temperature distribution of the proposed design was investigated. The air temperature impact, relative humidity, energy consumption, and the cooling air flow rate were examined. The increase in air temperatures and relative humidity in a very warm climate were shown to produce high water yield and productivity. The use of fins on both sides of Peltier also resulted in high water production. Maximum water generated was 20 mL/h at an airflow speed of 1 m/s (Fig. 8).

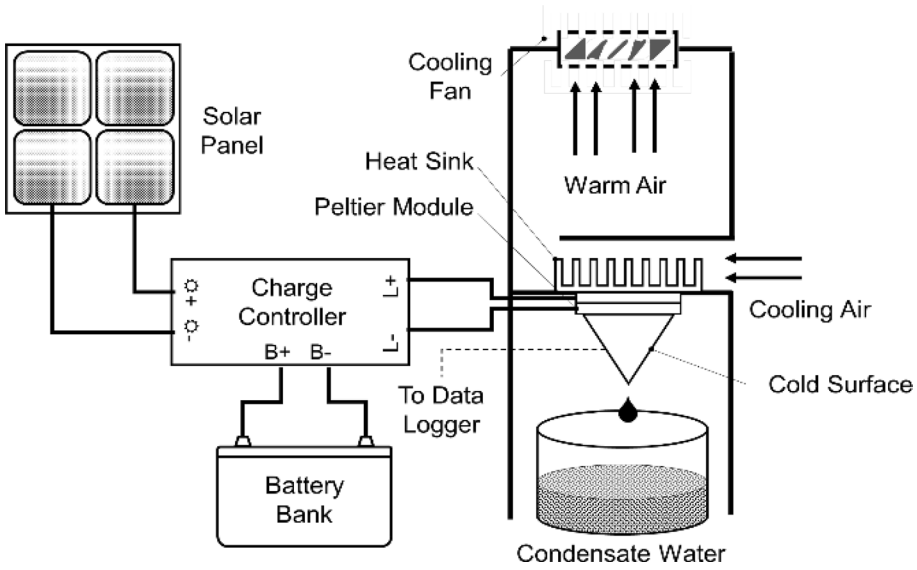

Fig. 8 Schematic representation of a solar-powered thermo-electric AWG by Kadhim et al. (2020)

Absorption–adsorption–desorption type (passive AWG)

Primitive dry desiccants

Passive AWGs do not require electrical or mechanical power to generate the net water generating effect. The desiccants can be of many types; solid, liquid, or composite desiccant depending on the use and climatic conditions of the area of utilization. In the absorption–desorption cycle, water from the atmosphere is absorbed by a suitable desiccant material placed inside the AWG, as the air comes in contact with it. Usually, this process of the cycle takes place during night time when the temperature is minimal and the humidity is high. After the moisture has been absorbed, the desiccant is exposed to sunlight, and the moisture evaporates and accumulates on the glass surface, which is then collected in a beaker or a tank. The glass cover in this case acts as a condenser (Wang et al. 2019).

The search for an optimized desiccant has continued and various desiccants have been tested experimentally to increase the water yield of the Passive AWG as in Milani et al. (2014). For this purpose, a prototype was fabricated utilizing the adsorption material phenomenon coupled with a low-temperature heat source. Further, solar plate collectors were installed on the prototype turning it into a completely passive system from Trinchieri (2019).

There have been some conventional desiccant systems employed for capturing the moisture from the ambient air by utilizing silicates like silica gel, but the main problem with silicates are their slow kinetics and the requirement of high

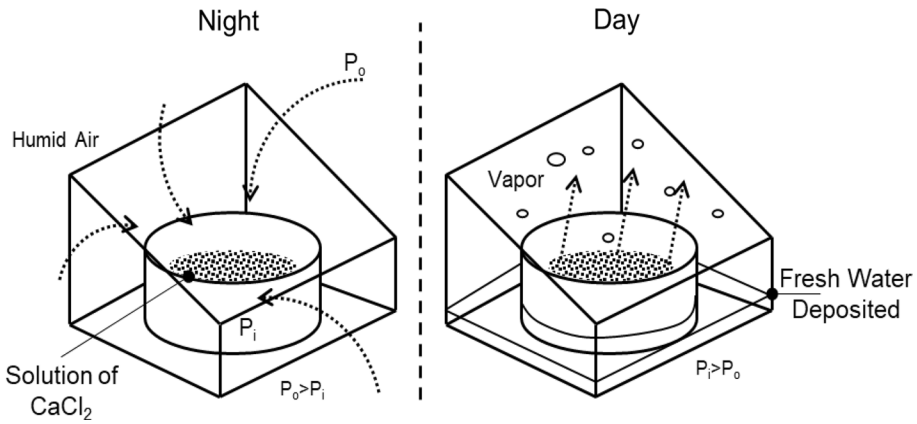

Fig. 9 Night-sorption day-desorption cycle (reproduced from Wang et al. (2019))

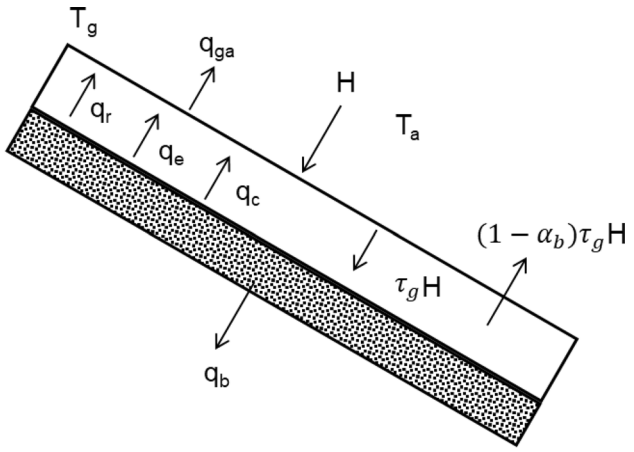

Fig. 10 Energy flow diagram of the sandy bed solar collector in Kabeel (2006)

temperature for the desorption phase (Zeng et al. 2014; Yuan et al. 2016) (Fig. 9).

Liquid desiccants

In a study by Sultan (2004), a non-conventional AWG system utilizing liquid desiccant impregnated in a cloth material as an absorbing material was designed and experimentally analyzed to determine the system efficiency. The system efficiency was shown to rise with the starting concentration, and decline when the regeneration air speed and absorption temperature were increased.

A solar collector infused with 30% concentration $CaCl_2$ on a sandy bed was utilized in a research by Kabeel (2006) to generate water from the wet air at different tilt angles (15°, 20°, and 25°). The system comprised of multiple components and is illustrated in Fig. 10. The ratio of consumed energy (heat) to evaporate water to gross amount of light incident on the surface of glass was used to determine the efficiency of the proposed technology given by Eq. (10).

$$\eta = q_e/H \tag{10}$$

The results revealed that the system was experimentally feasible as 1.2 L of freshwater was collected per square meter per day. The system's productivity was increased at 25° tilt angle as compared to other tilt angles.

Metal-organic frameworks (MOFs)

Metal–organic framework (MOF) is another desiccant material that has been employed for passive AWGs because of its greater water capturing ability and lower generation temperatures. They also offer a higher change in water yield with a small change in temperature because of their step-like isotherm. A study was conducted in which (MOF)-801 $[Zr_6O_4(OH)_4(fumarate)_6]$ was utilized as a desiccant and an air-cooled desiccant-based AWG was fabricated. The device was operated in a dry climate having low relative humidity values (10–40%). The findings showed that for a complete cycle the manufactured gadget could generate 0.25 L/kg of water (Kim et al. 2018).

Desiccants with metallic organic frameworks (MOFs)

The use of halide salts and metal–organic framework (MOF) as desiccants has created more space to utilize this technology and the capacities have been pushed to more than 100% of the weight of the desiccant, however, their costs remain a big concern (Wang et al. 2016; Henninger et al. 2017).

To increase awareness of the desiccant-based AWGs, a desiccant material in Gupta (2018) was identified named as lithium oxide nanomaterial; more precisely, Lithium Aluminate ($LiAlO_2$) nanopowder. Lithium Aluminate is a promising desiccant material and by utilizing samples of surface area (as low as 0.2 m^2/g), the amount of adsorbed water is given as Eq. (11).

$$Q_{ad} = 2.6 \times 10^7 A P^{\frac{1}{2}} \times \exp(3200/RT) \tag{11}$$

This desiccant material possesses ultra-fast kinetics (around 2–5 min), low-temperature desorption (approximately 60–80 °C), and costs less ($20/kg). The kinetics of $LiAlO_2$ is extremely fast, in the order of minutes as compared to other desiccants which have their orders in hours. Table 4 shows the adsorption times of some popular desiccants in comparison with Lithium Aluminate.

Nano-composite desiccants

A new technique that has caught the attention of researchers over the years is the use of composite desiccants for the

Table 4 Adsorption time (75% RH, 25 °C DBT) showing the extremely favorable kinetics of LAO vs some commercial desiccants in Gupta (2018)

Desiccant	Capacity % w/w	Time	Units
Silica gel	33	5.5	Hours
Bentonite clay	25	7	Hours
Molecular sieve	21	3	Hours
Calcium sulfate	10	4	Hours
Calcium oxide	5	10	Hours
LAO ($LiAlO_2$)	16	120	Seconds

dehumidification of air. The composite desiccant method is very similar to the working of liquid desiccant where the brine solution is exposed to open air and it adsorbs water vapor which is then transferred to the regenerator where it is converted to water. The only difference between the two is that the latter uses the composite desiccant to absorb moisture from the air. By the use of this technology, moisture adsorption takes place during the night whereas regeneration activity takes place during the daytime. This process can be cost-effective as it can utilize the energy from the sun to produce the desired product (water) which then can be collected into any reservoir (Nørskov et al. 2002).

The search for optimized desiccants has been a matter of concern for researchers over the past few years and it has resulted in several outcomes. The optimized desiccant should have a high capacity for water absorption, a reduced desorption temperature, and low cost. The modified sodium alginate was utilized in one beneficial study by Entazari et al. (2020), which utilized G and M block elements having cations that were more hydrophilic (e.g., Li and Ca). In addition, the hydrogel structure was embedded with carbon nanotubes to increase the adsorption capacity. It was revealed that this binary composite was able to take in 5.6 g of water for each gram of desiccant used in the experiment.

Mulchandani et al. (2020) employed nano-enabled desiccant coated with silica and photothermal CB NPs for absorbing water vapor from atmospheric air at low humidity. NP-SiO_2 desiccant increased the number of adsorption–desorption cycles for the 12 h cycle which ultimately resulted in higher water yield. A 5 wt% CB-SiO_2 desiccant yielded 0.562 g H_2O/g desiccant at an RH of 40% which was greater in magnitude than Silica Gel.

Polymers

Another technique under investigation is the development of a small microfluidic air-water generator based on PDMS (Polydimethylsiloxane), a polymer with particular chemical characteristics, limited water permeability, and high electrical conductivity. In 10 min, this gadget generated 0.2 mL of water in Wang et al. (2015)

Hydrogels

Hydrogels are gelatinous substances from 3D nanomaterial family which are able to swell in, and hold water. Jiao et al (2015) fabricated a Reduced Graphene Oxide Nanosheet Hydrogel RGO/CS/Ag which showed excellent results for dye degradation in wastewater application for two types of dyes. This suggested attractive potential of hydrogels in water generation, for use as an adsorbent.

Researchers have directed their attention toward the use of hydrogels in AWGs as they could be a very cheaper source to harvest water from the air as compared to other desalination processes. The study by Salehi et al. (2020a, b) concluded that hydrogel had many benefits but still required improvement in terms of strength and long-term stability for practical use.

To enhance the absorption capability of the sorbent material, an experimental study was conducted by Li et al. (2018) on an "easy-to-assemble-at-household" prototype utilizing a flexible hybrid photothermal water adsorbent comprising of deliquescent salt and hydrogel to elevate the water-absorbing capacity of a passive AWG from the atmosphere even in low humidity regions. Under natural sunlight, the device was able to generate 20 g of freshwater in 2.5 h, demonstrating that the hybrid hydrogel had exceptional water sorption capabilities.

To collect water from the air, a novel solid desiccant material was developed by Mittal et al. (2020). It comprised of super porous hydrogel (SPHs) of polyacrylamide (PAM) and AQSOA-Z02 zeolite. The hydrogel was successfully

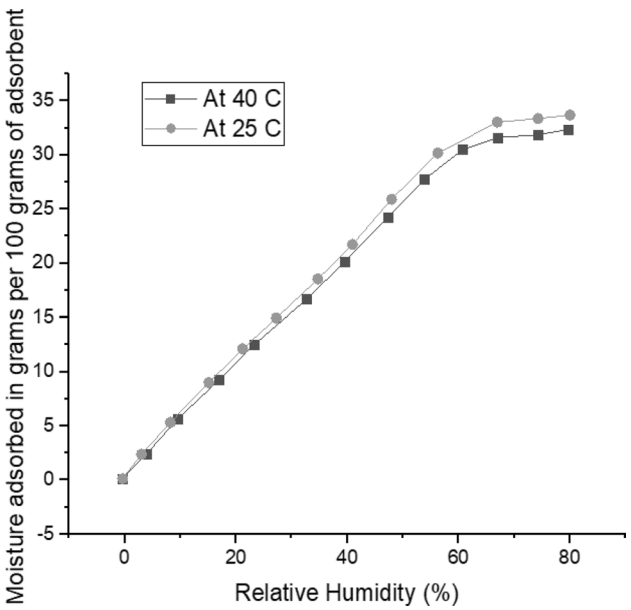

Fig. 11 Moisture adsorption of silica gel vs relative humidity (Sleiti et al. 2021)

Table 5 Comparison of performance of two models utilizing different Adsorbents by Sleiti et al. (2021)

Conditions and outcomes of the test	Model evaluation				Current evaluation			
Radiant energy (W/m^2)	558	792	558	792	509	529	556	529
Adsorbent	MOF-801/G				Silica gel			
RH at start (%)	30		30		40	30	40	40
Temperature of adsorbent at start (°C)	18		18		20			
Time of capture (h)	16.5		16.5		6			
Time of release (h)	7.5		7.5		6			
Mass of adsorbent (kg)	1.650		0.825		2.54	2.552	2.542	1.186
Output (g)	25	56	37	78	59	285	159	286
Relative productivity (g/kg)	15	34	45	95	23	112	63	241

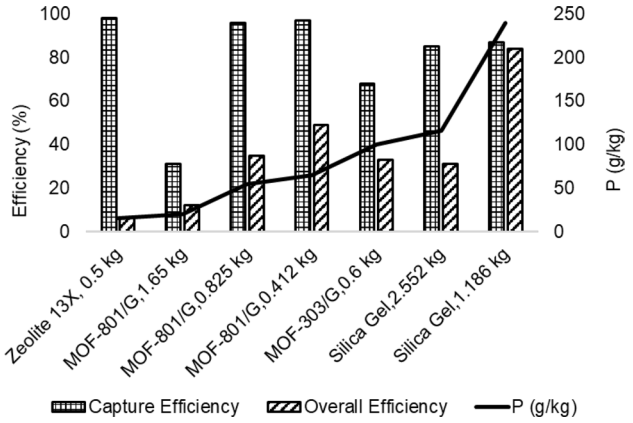

Fig. 12 Comparison of water yield and efficiency of various desiccants (Sleiti et al. 2021)

synthesized by techniques of gas blowing and foaming incorporating the zeolite particles with polymer matrix. Desiccant produced encouraging results and may be used in a variety of industrial settings.

Comparative studies in passive AWG

Silica gel versus MOFs

The use of silica gel as an adsorbent is quite common in our daily lives because of its outstanding moisture absorbing capability. Silica gel can absorb moisture approximately 50% of its weight in water. When relative humidity is low (below 30%), silica gel has a very poor moisture adsorption properties (16 g water per 100 g silica gel), however at increasing RH values, its moisture adsorption efficiency rises. Hence, it is useful in areas having RH greater than 50% as shown in Fig. 11.

To realize silica gel's adsorption potential, a prototype was fabricated and analyzed by Sleiti et al. (2021) under different conditions, and then compared with a reference experiment by utilizing metal–organic frameworks as adsorbent. For meaningful comparison, relative productivity (P) was defined for the system in terms of the amount of accumulated water and the amount of adsorbent.

$$P = m_{\mathrm{col}}/m_{\mathrm{sorb}} \tag{12}$$

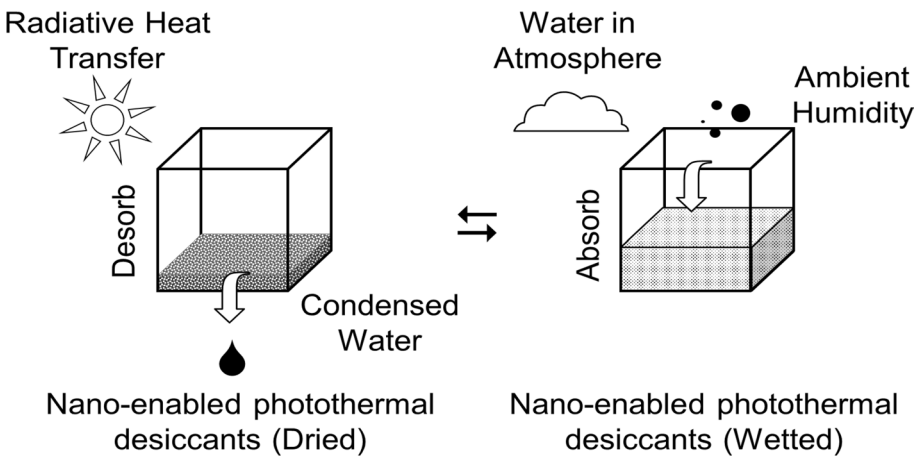

Fig. 13 Absorption desorption cycle utilizing nano-enabled photothermal desiccants (Mulchandani et al. 2020)

The findings of the two studies are compared in Table 5. The findings showed that as the relative humidity rose, so did the water yield (Figs. 12).

Further mentions of copper, aluminum, and zeolites in the literature

An air–water generator was designed and developed by Yang et al. (2020) which used a Cu complex as an adsorbent. This complex had a peak water consumption of about 300% and a high output water percentage. The fabricated model was named SMART FARM and mainly targeted the use of AWG in the field of agriculture. The system used solar energy for operation.

Over the years, the solar-powered adsorption-based AWG has been suffering from a major problem of low water productivity due to restraints in heat and mass transmission. For this purpose, research was conducted in which a dual-stage device was proposed by LaPotin et al. (2021) to enhance the water output via reusing the latent heat of condensation. An 18% increase in efficiency was observed over the single-stage adsorption-based AWG.

It was also revealed in Yang et al. (2020) that the aluminum content in zeolites was an essential component for the adsorption process for effective production. It was also recognized that the ZJNU-30 metal–organic framework was an appropriate possibility for cooling implementations due to its water capability, cooling capability, and coefficient of performance.

Utilizing an anhydrate salt for harvesting water from ambient air was also proposed and a Passive AWG was developed using $CuCl_2$ filled CNT coated mesoporous silica as an adsorbent in Alsaedi (2018). The powder could desorb 25 kg of water per 100 kg of water which was used in about 2 h. In addition, the system used solar energy for desorption. The system worked in the day and night cycles.

Silica gel versus nano-enabled photothermal desiccants

It is well known that the silica gel (SiO_2) in its solid phase may capture and hold water vapor in a variety of settings with varying relative humidity (20–100%) and temperatures (20–4 °C). The AWG system can only perform one adsorption–desorption–condensation cycle each day because it takes several hours of sunshine to generate enough heat to evaporate the adsorbed water vapor from silica gel. The application of nano-enabled photothermal desiccants on SiO_2 demonstrated that the AWG cycles per day could be enhanced, resulting in a higher desiccant surface temperature, by providing targeted heat sources. When nano-enabled photothermal desiccants were employed instead of SiO_2 alone, water output increased by a factor of ten in Mulchandani et al. (2020) (Fig. 13).

Calcium chloride with nano-enabled photothermal desiccants

$CaCl_2$ is another desiccant substance that has good absorption and desorption properties, and also works in areas having low humidity (RH < 20%). An air–water generator was set up using $CaCl_2$ as a deliquescent salt which adsorbed followed by an engineered- photothermal nanocomposite sheet (EPNS) by Namboorimadathil et al. (2020). The water produced was pure and safe for drinking. This technology of AWG was reported to work even in areas where other technologies were likely to fail. It was reported a cost-effective and efficient answer to the scarcity of drinking water. The whole setup was tested under a solar simulator where it gave a high (90%) solar to thermal conversion efficiency.

Nano-engineered aerogels

An optimized desiccant is the one that works best even in low humid areas. The utilization of Nano-Structured Biopolymer Hygroscopic Aerogels (NBHA) for atmospheric water generation was considered for that purpose by Wang et al. (2021). In this process, the NBHA was exposed to air for 60 h for moisture absorption. The mass change was recorded after every hour. The water uptake of the NBHA after the absorption process had taken place was calculated using Eq. (13).

It was found out that the NBHAs had very good moisture adsorbing capacity and worked even in areas having low humidity (RH of ~ 18%). It also required minimal energy to convert light to vapor using sunlight.

$$\text{Water uptake} = (m_i - m_a)/m_a \tag{13}$$

The rate and efficiency of evaporation of the NBHA was calculated from Eq. (14,15).

$$\text{Evaporation rate} = (m_b - m_c)/(A_1 \times T_P) \tag{14}$$

$$\text{Evaporation efficiency} = (m_b - m_c)/m_d \tag{15}$$

Water selective membranes

Before the cooling process, water vapor selective membranes were explored to split water vapor from several other

gases by Bergmair et al. (2014). The membrane's driving potential was partial pressure differential across the membrane. It was discovered that the energy required to remove water from humid air was reduced by more than half using a water selective membrane.

Reported improvements and economics of desiccants

Improvement in adsorption capability

The most important consideration for the efficiency of AWGs is the adsorption capacity of water. It was observed in Ejain et al. (2020) that LiCl (Lithium Chloride) had a high adsorption rate of water but a small deliquescent relative humidity (DRH). Due to this reason, a host was involved in building a steady and robust composite.

Generally, the composite materials are economically viable, have good working characteristics, and are stable (Wang et al. 2017). Salts turning into aqueous form on adsorbing moisture may be successfully employed for an AWG by choosing the right host matrix. ACF is a familiar adsorbent because of its uniform porosity distribution and short diffusion distance in numerous applications (Suzuki 1994). The water holding capability of ACF is not good but its structure and brittle nature of fibers makes it a suitable candidate to use as a host matrix. With the same salt $CaCl_2$, the adsorption capacity is higher than silica gel (Wang et al. 2016).

To improve the adsorption capability, Ejain et al. (2020) LiCl salt was combined with magnesium sulfate. Both these salts had different characteristics. $MgSO_4$ increased the water adsorbing capability and it was reported that a single molecule of magnesium sulfate had the ability to hold up to seven molecules while the remaining being in solid state. The purpose of this combination was to increase the adsorbent capacity and simultaneously decrease the possibility of leakage. The results revealed that the adsorption rate increased by the multi-stage inclusion of $MgSO_4$. At greater humidity conditions, the produced prototype from the chosen composite exhibited reduced AWG intensity. At an RH of 35%, the design produced water-to-adsorbent weight ratio of 0.92 when evaluated in dry climatic circumstances.

Improvement in desorption capability

Various attempts have also been made to enhance the desorption capabilities of an air-water generator in order to boost freshwater output, such as in Wang et al. (2019). They used a high-concentration liquid sorbent in combination with interfacial solar heating based on a salt-resistant GO-based aerogel that served as solar heat absorber. At an RH of 70%, it was discovered that water output was improved by 2.89 kg-m^2/day when using interfacial solar heating with a liquid sorbent concentration of 50 wt% $CaCl_2$ solution. This cost-effective and dependable method provided an appealing approach and relief to areas facing water scarcity, by collecting water from the air.

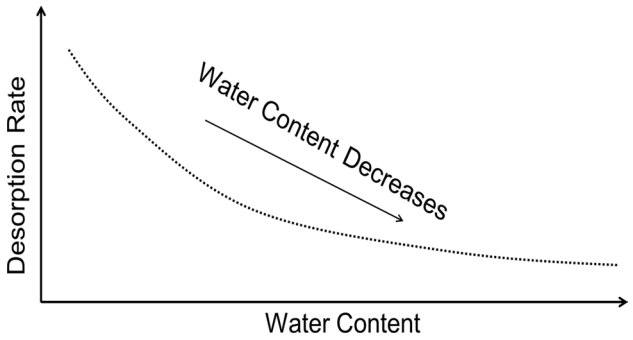

Fig. 14 General trend of desorption rate of water of conventional AWG (reproduced from Qi et al. 2019)

A limiting factor for final water output is insufficient desorption during the daytime. Figure 14 shows the desorption rate of water in a conventional AWG. An AWG was, therefore, fabricated by Qi et al. (2019) in which both the absorption–desorption processes took place simultaneously, as is illustrated in Fig. 15, to enhance the desorption capability of the generator and stabilize the water quantity in the sorbent. It was revealed that this prototype of AWG enabled water generation at a high pace for the outdoor environment. (Fig. 15).

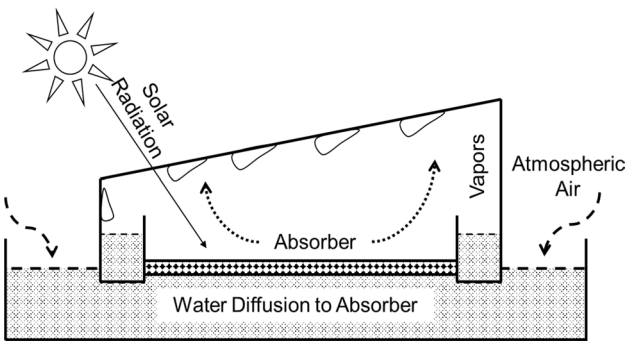

Fig. 15 Schematic illustration of the interfacial solar driven AWG by Qi et al. (2019)

Table 6 Comparison of annual water yield vs annual cost of commercial desiccants with currency in USD (Srivastava and Yadav 2018)

Desiccant	Annual water yield (L)	Annual cost (USD)	Payback period (years)
Silica gel	56.57	0.3649	6.40
Molecular sieve	15.69	1.3299	6.40
Activated alumina	13.87	1.4763	6.38
LiCl/river sand	32.85	0.6419	6.39
LiBr/river sand	26.64	0.7811	6.38
$CaCl_2$/river sand	41.97	0.4796	6.41

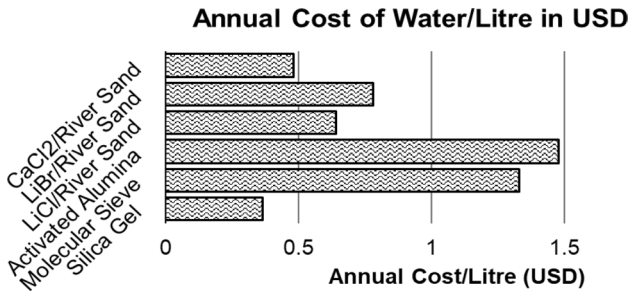

Fig. 16 Water cost per liter on an annual basis of some popular desiccants (Srivastava and Yadav 2018)

Economic viability of desiccants

Different desiccant materials were used in economic assessment of generating water from the air, and composites were tested by Srivastava and Yadav (2018) (Table 6). Scheffler reflector is a concentrator having a fixed focus. It focuses the sunlight at a specific point by utilizing portion of the paraboloid. Six cases were studied. They are illustrated in Fig. 16 and silica gel was found to be the most economical desiccant. The annual cost was calculated using Eq. (16).

$$\text{Annual cost/litre(USD)} = \text{Annual desiccant cost/Annual water harvesting} \quad (16)$$

Solar stills and embedded passive AWG

Sustainable and efficient desalinating systems have become the most important need of the world today. The problem of water scarcity can be overcome by using these systems; solar still being one of them. Solar stills provide distilled fresh water from saline/brackish water by simple means, requiring less or no energy (Kabeel et al. 2017; Abdullah et al. 2018). Solar Still can also be employed as an air–water generator by withdrawing water from the air utilizing the heat of the sun. There have been several geometries proposed and investigated for the optimization of solar stills in recent years. They are conventional (Kabeel et al. 2014), inclined (Kumar et al. 2017), pyramid (Nayi and Modi 2018), spherical (Modi et al. 2020), drum (Abdullah et al. 2019), stepped (Xiao et al. 2019), wick (Omara et al. 2015), and tubular (Panchal et al. 2019).

The effectiveness of TSS was examined, using black fabric and gravel as heat storage medium. A parabolic concentrator was also used to track the sun. It was found that the water yield improved by a significant amount by utilizing the modified design of TSS (Elashmawy 2017, 2020a, b). In the TSS, a black cotton cloth bed filled with $CaCl_2$ was utilized. During night, water output was determined by placing a fan for air circulation and operating at different speeds (Elashmawy 2020a, b).

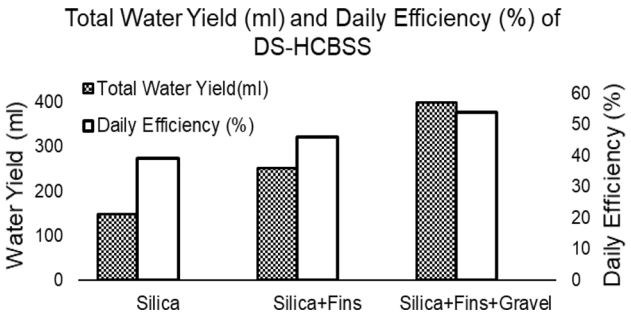

Fig. 17 Water yield and efficiency under three cases of Essa et al. (2020)

Table 7 Silica gel properties used in the experiment in Essa et al. (2020)

Density (kg/m^3)	Heat capacity (J/kg K)	Thermal conductivity (W/mK)	Specific surface area (m^3/g)	Nominal pore diameter (nm)	Pore volume (ml/g)	Water adsorption capacity (25 °C and 50% RH)
776	1073	0.1	700	2	0.4	25%

The performance of DS-HCBSS employing silica gel as an adsorbent was investigated in another experimental setting. Table 7 lists the characteristics of the silica gel, which was utilized in this experiment. In an experimental research by Essa et al. (2020), three instances were explored which are illustrated in Fig. 17 The water yield increased significantly in the third case.

In low humid regions, the AWG potential was explored using the five-stage trapezoidal prism solar still by Elashmawy and Alatawi (2020). The racks were soaked with calcium chloride solution, containing black cotton clothes. The manufactured prototype's thermal and yield efficiency were given as the amount of energy utilized to yield water and overall energy taken from sun. They are displayed with Eq. (17, 18). With solar power of 22.96 MJ/L the findings showed a water output of 1.06 L/m^2.

$$\eta_{ev} = (m_{ev} \times h_{fg})/\mathrm{IA}_2 \tag{17}$$

$$\eta_{\mathrm{Yield}} = (\mathrm{Yield} \times h_{fg})/\mathrm{IA}_2 \tag{18}$$

Water generation from fuel cells

In the previous discussion, several approaches for the creation of air water were discussed. However, the technology utilized must be energy efficient. Hydrogen and oxygen were utilized in an electrochemical process in a fuel cell to produce energy and water (Liso et al. 2016). Since water is produced by fuel cell as a by-product, it is utilized in different applications all over the world (Mekhilef et al. 2012). The by-product water from the fuel cell can be recovered by dehumidification process. The recovery of liquid water from the fuel cell stack had been previously employed in a space shuttle (Orta et al. 1998). The water obtained from this recovery technique could only be utilized if it fulfils the requirement of the WHO. Therefore, water quality was compared by using two commercially available FC namely the LTPEMFC and MCFC by Tibaquirá et al. (2011). It was revealed that the latter failed to fulfill the quality requirements of drinking water set by the WHO. It was also determined that the likelihood of flooding was greatly reduced by using this water recovery technique in the fuel cell stack (Chen et al. 2015; Zhang et al. 2017). The idea of utilizing fuel cells in AWGs came into play due to technology optimization (Salehi et al. 2020a, b). Thus, a hybrid model was proposed comprising of a fuel cell and an AWG which increased the yield of freshwater production without consuming much energy of an AWG by Kwan et al. (2020a, b). Under 70% relative humidity and 500 W compressor power, the freshwater yield increased by 1 kg/h.

A fuel cell is said to be the primary engine of electric vehicles (Khaligh and Li 2010). Apart from these applications, the fuel cell can also be utilized as a micro grid energy source (Mane et al. 2016). The operating efficiency of fuel cell has been found as 50% by Al-Fulaij 2011 and the remaining 50% is considered as waste heat. It was proposed to employ this waste heat in the liquid sorbent production process to extract the ingested water vapor as condensed water by Kwan et al. (2020a, b). (Fig. 18).

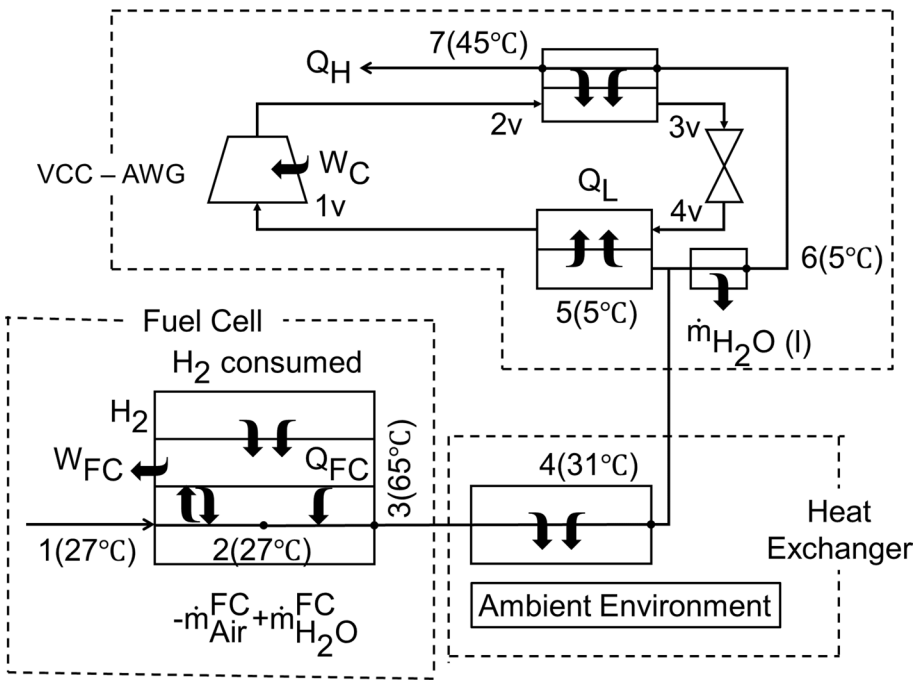

Fig. 18 Schematic depiction of the hybrid system of FC-AWG (Kwan et al. 2020a, b)

The use of microbial cell technology for producing energy and purifing water

Microbial Cells, like AWGs, are emerging technologies that purify waste water rich in organic compounds while simultaneously creating sustainable energy and supplying potable water for everyday use. The mention of MFC in power generation can be found with promising results in the literature. Tran et al. (2021) produced a study of 4 MFCs constructed which underwent test for 17 weeks. The performance of all MFC replicates became stable after 9th week while inoculating with domestic waste water with a ratio 1:4 between primary sedimentation and activated sludge. The study like these emphasize on water conservation and opens new venues for an integrated approach, reusing waste-water as power generating core for atmospheric water generation.

Microbial fuel cell (MFC)

Many researchers have focused their efforts on waste disposal into the environment, and their concern about pollution has driven them to develop a plethora of technologies and ways to address this issue. To accomplish this purpose, researchers have worked on a number of environmental pollutants, among which included the treatment of agro-industrial waste water to address the aforementioned issue. An effective agro-waste treatment structure can recover energy while stabilizing waste simultaneously, and (MFC) Microbial Fuel Cell is one of the promising technologies that can produce energy while also treating wastewater (Pandit et al. 2021). MFC is a bioelectrochemical system that enables the conversion of organic matter to energy from a large number of complex carbon-based compounds. This is accomplished by harnessing the action of microbes on waste to produce electrical energy. A conventional MFC is made up of two chambers, an anode and a cathode for oxidation reduction processes, with the chambers commonly separated by an anion exchange membrane (IEM) demonstrated in Fig. 19 (Pandit et al. 2021).

The use of various agricultural wastes and wastewater containing various industrial by-products to generate bioelectricity in MFC appears to be a potential and alternative source of renewable energy generation and variety of agricultural wastes and wastewater may be used to boost bioenergy production utilizing a variety of MFCs. Hence, agro-waste can be converted to bioenergy using both biochemical and thermochemical MFC methods (Pandit et al. 2021).

In MFCs, the anode is made up of carbon-based material which limits the anodic performance of the anode due to its low conductivity. The anodic performance of the carbon-based anode can be enhanced by applying corrosion-resistive current collector on the anode. In a single chamber MFC, two distinct carbon-felt anodes with titanium wires (CF-W) or stainless steel mesh (CF-M) as current collectors were examined by Jung et al. (2018) on the basis of the hypothesis that anodic performance would improve by increasing metal current collector. It was observed that the CF-M with the larger current collector area (21.7 cm^2) increased maximum power by one-third, up to 2311 mW/m^2, decreased anodic resistance down to 81%, and anodic impedance by 92% in short-term testing such as polarization and impedance tests. In long-term tests, it was noted that the CF-W with the smaller current collector area (0.6 cm^2) outperformed the others in terms of power and current generation. Therefore,

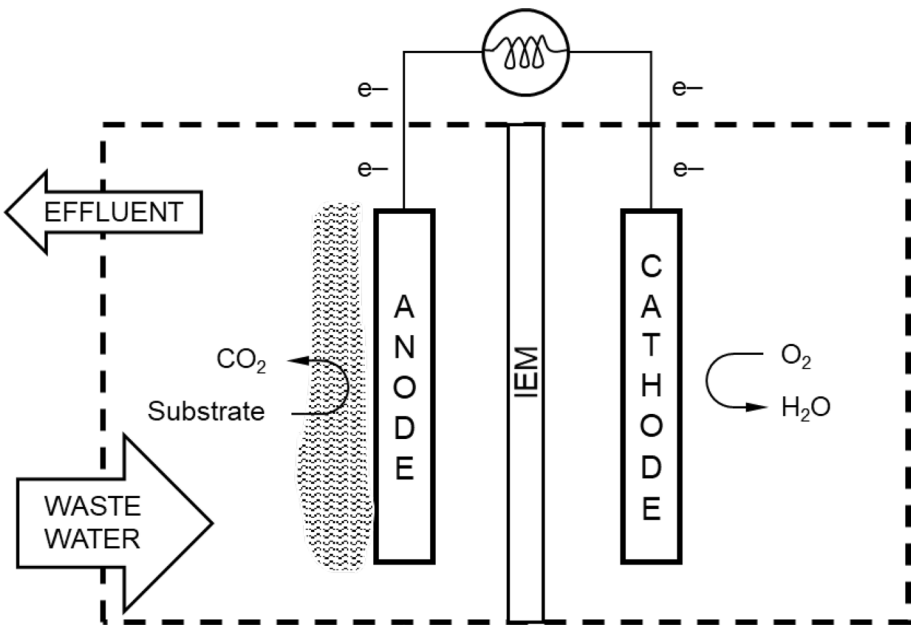

Fig. 19 Schematic of dual chamber MFC experimental setup (Pandit et al., 2021)

it was suggested that a larger current collector would be beneficial in the short term but detrimental in long term, since larger current collector was helpful for current but hindered mass transfer and microbial development (Jung et al. 2018).

Brushes were tested in various arrangements by Nam et al. (2020) using MFCs for energy production and waste water treatment. Cell performance was improved owing to reduced electrode resistance when anodes were added to the horizontal layout. Maximum power, with four anodes, increased three folds compared to the increase with two anodes. Anode polarization, with four anodes, decreased more than that with two anodes. Current was found to increase by four times in selective arrangements. It was further demonstrated that increase in electrical input had a direct impact on current generation, but inverse on diffusion resistance. Installation of multiple anodes horizontally along cathode in different rows was recommended. With external power supply, they also suggested installing multiple anodes both horizontally and vertically. A similar study on brush-anode configurations on performance of MFC showed increase in current densities by as much as 30% whereas power by 20% (Kang et al. 2017a, b).

In the air cathode of MFCs, the catalyst used for the oxidation reduction reaction is (AC) Activated Carbon because it is an inexpensive catalyst. However, performance improvement of AC is essential as it has a low electrochemical catalytic activity. Therefore (MOF) metal–organic frame work was introduced as a catalyst with improved electrochemical catalytic activity.

Koo and Jung (2021) employed ultrasonication (U) along with solution precipitation (H) to combine ZIF-67 (cobalt-nitrogen framework) with activated carbon to create ZIF-67U and ZIF-67H cathodes and tested in MCFs, respectively. The former produced 4203 mW/m^2 whereas the later produced 3881 mW/m^2, which in comparison with 2625 mW/m^2 (for AC cathode), were found 60% and 48% higher. The performances, in power density, of the two cathodes, were also found to exceed that of Pt cathode by 160% and 140%. The cobalt-nitrogen test revealed an increase in the active site of the oxygen reduction reaction (ORR), increased the reaction rate, and decreased charge transfer impedance.

MOF is a good substitute for (AC) Activated carbon as a catalyst in MFCs, but AC is more cost effective than MOF, so Koo et al. (2019) worked on increasing the cathodic performance of AC by replacing (CB) Carbon Black, which was utilized as a conductive supporting material in AC with reduced graphene oxide (rGO) in an optimum ratio, where rGO replaced CB in the following weight ratios: 0:30 (rGO0); 5:25 (rGO5); 15:15 (rGO15); 30:0 (rGO:CB) (rGO30).

Following the completion of the experiments, cathodic performance was found to increase with the best rGO additions, while decreasing cathodic resistance. Similarly, inclusion of rGO enhanced cathodic performance due to its geometry and better electrical conductivity than CB. However, cathodic performance was reduced for complete replacement of CB with rGO due to larger thickness and the morphological structure. Thus, cathodic performance could be increased and electrical power generation of MFCs can be enhanced by optimizing rGO.

Microbial reverse electro dialysis cell (MRC)

MFC and a reverse electro dialysis (RED) stack are combined to form a microbial reverse electro dialysis cell (MRC) for treating wastewater and generating power from salinity gradient between seawater and fresh water. Furthermore, in an MRC, power generation can be considerably increased. It is critical to operate an MRC at an optimal flow rate to RED since it is linked to energy production rate and economic feasibility. Therefore the influence of RED flow rates were tested on the electro chemistry, performance and power production in MRCs. Four distinct flow rates of high and low concentration solutions were investigated for this purpose. 10 mL/min (3.71 W/m^2) had the highest maximum power density, whereas 7.5 mL/min (5.36 A/m^2) had the highest optimum current density. Following the examination, significant differences were not found between power generation at 7.5 mL/min and 10 mL/min. However, 7.5 mL/min was preferable for production. The same flow rate of RED was chosen as the best option for MRC operation (Kang et al. 2017a, b).

Microbial desalination cell (MDC)

Researchers have proposed various desalination-based solutions to overcome the shortage of drinking water, including reverse osmosis membranes and Microbial Desalination Cells (MDC). MDC is a new type of desalination technology that aims to produce enough drinkable water for daily use. MDC are microbial consortia that remove ions from low-salinity aqueous solutions using chemical energy shown in Fig. 20. This review outlines the working principle of MDCs, more frequently used MDC cell layouts, and the factors which significantly effect the performance. The paper also includes a techno-economic analysis and lifecycle assessment of microbial desalination systems, as well as descriptions of electrode manufacture and genetic manipulation procedures that could improve MDCs performance (Zahid et al. 2022).

Microbial electrolysis cell (MEC)

The increased global warming caused by carbon and methane escaping into the environment as a result of the

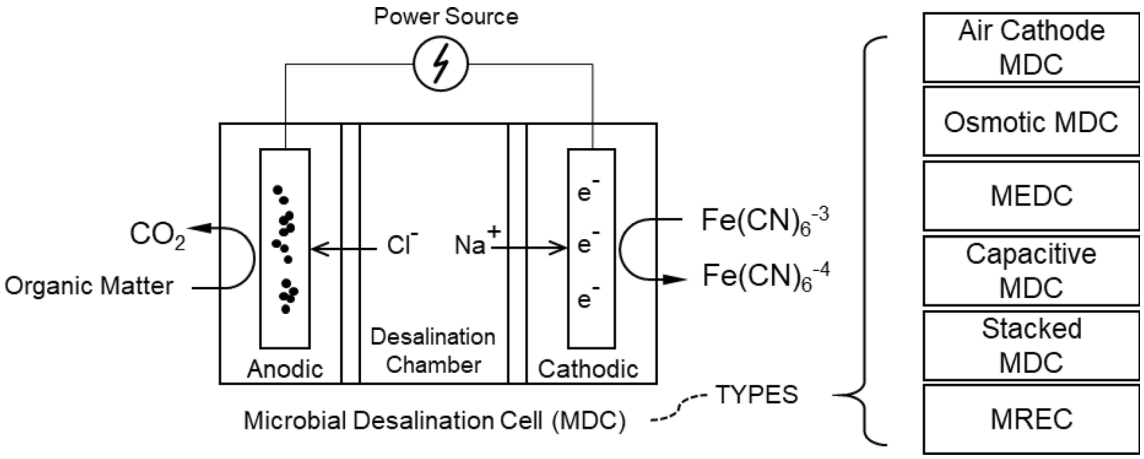

Fig. 20 Water desalination process using MDC (Zahid et al. 2022)

conventional methane production process has prompted the development of green and sustainable methane production technologies, such as the MEC (Microbial Electrolysis Cell). MECs are created from the (MES) Microbial Electrochemical System. Electrical energy in MES is generated, via the reduction–oxidation process, transforming the chemical energy extracted from waste lignocellulosic biomass and wastewater. It is a novel technology that decomposes organic matter and produces hydrogen at anode and cathode respectively (Son et al. 2021).

MECs that produce methane are made up of four key parts: anode, bio cathode, separator, and electrical source Fig. 21. An oxidation reaction occurs at the anode, which is required to provide electrons for CO_2 reduction in the bio-cathode region. Second, the bio cathode is a key component in which methane is created by microorganisms using electrons supplied by the anode's oxidation reaction. To keep the solution electro neutral, a separator or ion exchange membrane is required for the movement of positively charged ions such as Na+, K+, and H+ from the anodic chamber to the cathodic chamber. Finally, externally supplied electrical energy is required to thermodynamically drive the reaction (Amrut Pawar et al. 2020).

Amrut-Pawar et al. (2020) used various biochemical pathways to discuss MEC mechanism for electromethanogenesis, in which methane was produced in two ways: direct method through the uptake of electrons from electrode [Eq. (19)], or indirectly through production of hydrogen and other chemicals such as acetate and formate, which were created and mixed with carbon dioxide to form methane Eqs. 20 and 21 (Amrut-Pawar et al. 2020).

Direct electromethanogenesis:

$$CO_2 + 8H + 8e^- \rightarrow CH_4 + 2H_2O \quad (19)$$

Indirect electromethanogenesis:

$$2H + 2e^- \rightarrow H_2 \quad E = -0.41 \text{ V versus NHE} \quad (20)$$

$$CO_2 + 4H_2 \rightarrow CH_4 + 2H_2O \quad (21)$$

MECs require low energy input, have self-sustaining microbial biocatalysts, yield high conversion efficiency, cost less, and inhibit pollution.

To make the application of MECs economically viable (Son et al. 2021), used high performance and low-cost cathode materials and showed that the performance of MEC was effected by varying the cathode material. Five different cathodes made of activated carbon (AC) and nickel powder (Ni) as cathode catalyst; polytetrafluoroethylene (PTFE) and polyvinylidene fluoride (PVDF) as catalyst binder; stainless steel mesh (SSM) as cathode substrate, were tested in MECs. The best performing cathode was Ni/AC/PTFE, followed by Ni/AC/PVDF, AC/PVDF, flamed-oxidized SSM (SSM/F), and SSM. Maximum hydrogen production rate was found with Ni/AC/PTFE with hydrogen purity of 97.5%, coulombic efficiency 124%, energy efficiency 216%, cathodic capacitance 0.9924 F, and cathodic impedance 35Ω. Worst performance was found with SSM 71% hydrogen purity 71%, coulombic efficiency 36%, energy efficiency 62%, cathodic capacitance 0.0008 F, and cathodic impedance 62Ω.

Effect of climatic conditions and air flow

General spectrum of climatic conditions and AWG's performance

The water yield of the AWG is heavily influenced by climatic conditions. The higher the moisture content, the more water the AWG can produce. However, ideal situation doesn't exist

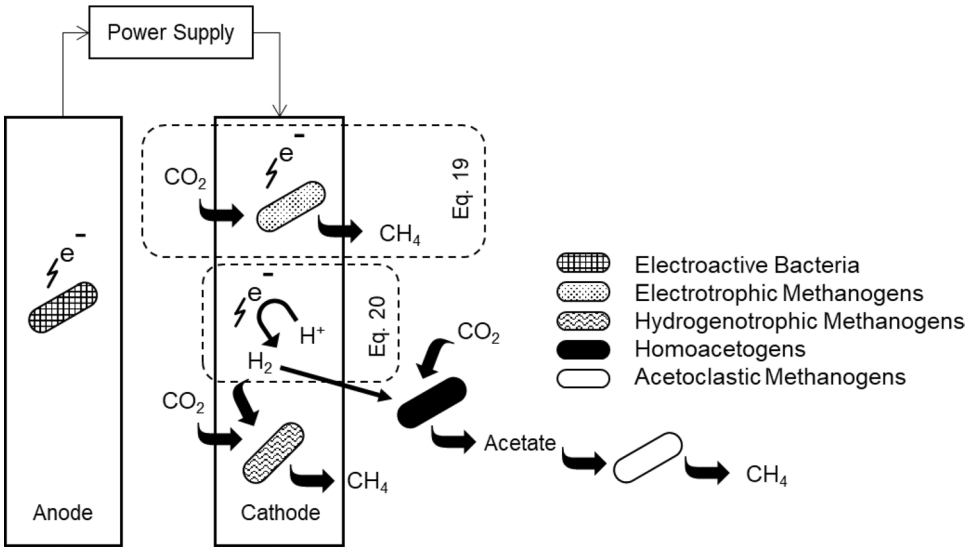

Fig. 21 Schematic of the process of (MEC) microbial electrolysis cell (Amrut-Pawar et al. 2020)

everywhere in the world. Hence, AWG under varying climatic conditions is reviewed in this section.

Various climate settings (Red Sea and Arabic Gulf in summers, Southern Europe in South Spain) have been used for the fabrication and testing of a solar thermoelectric AWG. It was shown that under all three weather situations, the prototype constructed in Kabeel et al. (2016) produced 3.9 L/h/m^2 fresh water with fan power not exceeding 9.1 W. The testing of AWG was also conducted by Patel et al. (2020) under various climate conditions across India and the globe. Seven different climatic conditions were put under investigation for which the temperature and RH conditions are shown in Table 8. The tests were carried out employing a climate chamber artificially. The AWG was working on the principle of the vapor compression cycle. The results showed that water yield increased when moisture humidity was high. The water yield rate ranged from 0.28 to 1.78 L/h. Electricity usage ranged from 0.75 to 4.71 kWh/L.

Another research by Patel et al. (2019) dealt with the analytical investigation of the AWG in the coastal regions of India. The amount of condensate generated was shown to be greatly dependent on the air humidity ratio and temperature. It was reported that approximately 2000 kg of condensate were obtained in a month from the coastal regions of India, equivalent to 70 kg/day (Table 9).

The performance of the evaporator unit of the cooling condensation type AWG was also analyzed under different climatic conditions by focusing on the rate of water condensed, and fruitful results were obtained. The findings suggested that AWG's effectiveness depends greatly on climate, and that the AWG system having a temperature of 15 °C and RH below 40% was inefficient. High-temperature climatic conditions were found favorable for the operation of the AWG (Herman et al. 2020). Coastal areas showed the highest water yield. For example, in Yemen (a water deprived country), coastal cities Aden and Hodeida had roughly 99% of the desired time for the operation of an AWG. Hence, it was concluded that humid and warm areas showed the best water yield for the AWG (Gido et al. 2016).

Experiments in literature

The volume of water produced as well as the condensation rate were varied using different intake air relative humidity

Table 8 Performance of AWG under varying climatic conditions (Patel et al., 2020)

Climate settings	Temperature	Rel. humidity	Output of water	Electricity consumption	Electricity price
No unit	(°C)	(%)	(L/h)	(kWh/L)	(USD/L)
Warm and humid	35	95	1.78	0.75	0.043
Mild and humid	25	75	0.61	2.04	0.116
Cold and humid	17	80	1.05	1.22	0.205
Warm and dry	40	27	0.28	4.71	0.268
Mild and dry	22	45	0.3	4.4	0.249
Mild only	22	50	0.35	4.11	0.233
Warm and mild humid	35	70	1.35	1.03	0.058

Table 9 Performance of AWG under varying climatic conditions (Patel et al. 2020)

Experiment	Flow rate (cu.m/h)	RH level (%)	Temperature (°C)	Water flow rate (g/h)	Rate of condensation (%)	Energy usage of water production per sq. m (kg/kWh)
A	29.7	67.8	24.3	11.2	2.42	0.889
B	29.7	77.7	23.1	15.2	3.08	1.207
C	29.7	84.7	24.2	22.3	3.87	1.771
D	29.7	92.7	23.6	25.1	4.10	1.993
E	29.7	86.8	21.9	18.2	3.56	1.445
F	50.4	86.5	22.1	18.7	2.13	1.485
G	70.6	86.5	21.2	20.6	1.76	1.636

and airflow speeds. As the RH increased, the amount of water and condensation percentage also increased. Water production increased with increasing airflow rates and decreasing condensation rates. At an average rate of 25.1 g/h, the largest quantity of produced water was 25.1 gm, which was equivalent to approx. 0.22 m^2 of condensation surface, and 58 W power input. It was compact and could function at a low air flow rate for applications where outdoor use was expected. This work was significant in helping to build and optimize a highly efficient portable water generator. These experiments evaluated the influence of different input relative humidity (RH) and modest airflow speeds on the produced water and condensation rate.

Cross-flow fans were used to adjust airflow rates. Various humidifiers were used to regulate the RH of the intake air. After flowing through the humidified air in an intake air channel, the inlet air was cooled to its dew point using TECs. The condensate droplets expanded to the size of raindrops and ultimately settled in the water pan. The hygro-thermographs were used to determine intake and exit air's RH and temperature. Thermocouples were utilized to examine the fin temperature (Liu et al. 2017). The rate of condensation η was calculated by Eq. (22).

$$\eta = \text{Generated water}/\text{Inlet moisture content} \tag{22}$$

Impact of relative humidity

Condensate water and condensation rate were found to be related to the RH level in the same experiment. Keeping inlet air temperature, flow rate, and input power unchanged, rise in moisture content was due to an increase in RH. The saturation points of the intake air increased with the RH. The lower the RH, the smaller became the gap between input air temperature and its dew point. When ΔT decreased, the process became easier to condense. Generally, increasing inlet relative humidity was favorable and created more water as well as a higher rate of condensation (Liu et al. 2017).

Impact of air flow rates

An experiment by Liu et al. 2017 was run using a range of flow rates to demonstrate water production, and the average produced water per hour was established after stabilizing the flow. The high temperature of fins was probably responsible for the fact that the water production is lower at a higher flow rate. It took around 8 h for the produced water to stabilize and then began to rise with higher flow rates. The fact that cold-side fin temperatures declined with time, as well as the growing flow rate, both caused the vapor concentration in the channel to increase.

As the input air flow rose, the water amount increased, but the condensation rate decreased. Increased airflow rate brought in more moisture, thus intensifying the disturbance. However, with a higher airflow rate, the condensation rate dropped, which limited the system's cooling capability. Since the flow rate was increased, there was less time between moist air and condensate contact surfaces. As a result, the condensation on the cold-side fins was significantly decreased, along with a reduction in the temperature difference between input and output air, possibly contributing to the lower rate of condensation. The condensation rate was increased due to extended contact time and continual cooling.

Condensation efficiency was lower and dropwise condensation resulted in heat transmission rates that were almost ten times higher than film condensation. Rising intake RH and inlet air flow rate caused a rise in the maximum quantity of produced water, which was approximately 25 g/h. When RH increased, the rate of condensation increased, but it dropped

with an increase in airflow. The primary causes for the low condensation efficiency were minimal capacity for cooling, minimal surface area for condensation, one-pass construction, and attachment of droplets to the surface of the condensate.

Efficiencies and cost effectiveness

Climatic efficiency

For the efficient evaluation of the Air–Water Generator, experiments were carried out in Vietnam by using detailed values of temperature and relative humidity for 24 h. The results suggested that the temperature at the outlet airflow throughout the evaporator should be 13 °C to produce 1 L of water with the minimum energy consumption (Martinez 2020).

System efficiency

As the amount of energy consumed varies on the air velocity and temperature, so does the overall efficiency of the recommended system. The amount of energy supplied to a forced air stream was found to increase with increasing air velocity. Increasing the air temperature also increased the system's energy usage. System effectiveness was given as the relation of usable heat produced by system and the total amount of heat needed to generate water (Nørskov et al. 2002).

$$h_{\text{sys}} = Q_v / Q_t \tag{23}$$

Cost effectiveness

AWG is a method for obtaining fresh and clean water but it should be cost-effective as well when compared with other water sources. A research was conducted which compared water price obtained from AWG with the price of bottled water by Asiabanpour et al. (2019). A 10-day trial of the AWG was conducted and data of the water yield and the power consumed was collected over a 24-h testing period. The water yield, power consumption, temperature, and relative humidity data for the 24-h testing period are shown in Table 10. AWG was determined to be more cost-effective.

Promotion of the AWG technology

Water quality

The presence of heavy metals in condensed water collected from AWGs was investigated. A total of 108 samples were collected in Bautista-Olivas et al. (2017) at three different locations in Mexico, and the quality of water was tested via mass spectrometry using inductively coupled plasma. The pH was analyzed via a potentiometer. The quantity of heavy metals in the condensed water was found to be under WHO consumption guidelines after analysis. The condensed vapor had trace elements that were of anthropogenic origin.

Urban normalization

To normalize the use of AWG in urban areas, experimental analysis was conducted on a commercially built AWG. It was revealed by Inbar et al. (2020) that the water produced by the AWG still fulfilled WHO drinking water standard in the urban environment where the contamination present in the atmosphere had changed the chemical composition of the dew.

An AWG prototype was built utilizing two Peltier devices to suffice an average family water needs while also meeting WHO drinking water quality standards and lowering energy consumption by using solar power instead of grid electricity in Dash et al. (2015). It was observed that the device was

Table 10 10-day test data of the AWG in Asiabanpour et al. (2019)

Day	Water yield (L)	Energy usage (kWh)	Average temp. (°C)	Higher temp. (°C)	Lower temp. (°C)	Average RH (%)	Higher RH (%)	Lower RH (%)
1	4.385	6.26	28.3	36.6	20	50.5	88	22
2	5.88	7.38	27.8	36.1	18.3	49.1	78	28
3	11.34	12.67	28.0	36.6	20	63.4	93	25
4	11.25	10.54	29.4	36.6	25	68.8	94	39
5	11.85	11.63	29.3	36.6	22.7	65.9	96	37
6	11.75	10.97	29.8	36.6	25	65.7	90	33
7	11.65	10.91	27.6	36.1	23.8	73.5	94	35
8	11.6	10.75	28.6	35.5	23.3	70.3	94	41
9	11.08	10.8	30.1	36.1	25.5	64.6	90	36
10	13.8	10.68	26.8	33.3	22.7	81.3	100	53

able to produce satisfactory results if the ambient temperature was 35 °C or more and relative humidity was above 50%. The quantity of water was calculated (in liters) in 1 cu. m of air at different relative humidity and temperatures. The humidity ratio and the amount of water are given by the following equations.

$$\text{Humidity ratio} = 0.622[(P_w)/(P_a - P_w)] \quad (24)$$

$$\text{Amount of water(L)} = \text{Humidity ratio} \times 1000 \quad (25)$$

Integrated system with rain water harvesting

Another idea was proposed in Gomez (2019) for designing a smart integrated water system incorporating the Rain Harvesting System (RHS) and Air-Water Generator (AWG) together for providing a possible solution to water scarcity. The results revealed that it could provide a steady solution for water generation.

Conclusion

One of the most pressing issues the globe faces today is the lack of water. To overcome this water drought, various methods and techniques have been proposed. One such technique is the generation of water from air. Cooling air beneath its dew point allows water extraction by dehumidifying air or, via use of desiccants by atmospheric water generation. The AWG can be both active and passive. Active mode requires the use of electricity whereas the passive mode works by utilizing energy from waste or renewable heat sources. Active technology predominantly utilizes the vapor compression cycle or the Peltier effect, unlike the passive AWG which works predominantly via the use of desiccants and solar radiation. This paper has reviewed all the techniques related to AWG. Comparison of Peltier and cooling condensation technique was presented in the paper and it was revealed that the latter was able to produce 8 times higher water yield than the former. The thermodynamic inspection of the Peltier was also carried out which showed that the rise in temperature of air flowing through the cold path of the thermoelectric coolers increased the water yield and the COP of the system but decreased the optimum airflow rate.

The Passive AWG was also discussed and reviewed in detail. Solar-powered AWGs comes in handy when there is an unavailability of electricity for the daily needs. A numerical model of the solar-powered AWG was developed and it was revealed that solar insolation, atmospheric temperature, and relative humidity had significant impacts on the output. Solar energy can also be utilized in the cooling condensation type of AWG and a prototype was developed which revealed that the prototype was able to produce 1 L of water per day. A solar-powered thermoelectric AWG model was also found set up in the literature and the results revealed that the maximum water generated was 20 mL/h. The passive AWG via absorption–desorption cycle was also presented which focused on the utilization of common desiccants as well as composite desiccants to increase the water yield of the AWG. The economic viability of some popular commercial desiccants was also presented and it was revealed that silica gel was the cheapest among them. Solar Still have also been developed greatly over the years because of its tendency to provide clean and fresh water. Hence, solar still assisted AWG is also a possible solution for the ever-growing water crisis. The performance of tubular solar still AWG and a DS-HCBSS AWG was also reviewed.

The technology utilized for the AWG must also be energy efficient and AWG employing fuel cells is a possible solution by recovering water via dehumidification process. The water obtained from fuel cell must fulfill the requirements set by the WHO and to test that, a comparison test between two fuel cells was found in the literature. It was revealed that the latter was unable to satisfy the recommended benchmark set by the WHO. The behavior of AWG under various climatic conditions was also reviewed briefly by comparing different climatic conditions and water yield of the AWG. The evaporator unit of the cooling condensation type AWG under different climatic conditions was also discussed. Some important atmospheric parameters (relative humidity, air flow rate) were considered to improve the water yield of AWG so that it can become a permanent solution for the ever-growing global water crisis.

Acknowledgments The authors wish to thank all who assisted in conducting this work.

Funding The authors did not receive support from any organization for the submitted work.

Declarations

Conflict of interest The authors have no conflict of interest.

Ethical Approval This article does not contain any studies with human participants or animals performed by any of the authors.

References

Abdul-Wahab SA (2008) Reviewing fog water collection worldwide and in Oman. Int J Environ Stud. https://doi.org/10.1080/00207230802149983

Abdullah AS, Essa FA, Omara ZM, Bek MA (2018) Performance evaluation of a humidification-dehumidification unit integrated with wick solar stills under different operating conditions. Desalination 441:52–61. https://doi.org/10.1016/j.desal.2018.04.024

Abdullah AS, Essa FA, Omara ZM, Rashid Y, Hadj-Taieb L, Abdelaziz GB et al (2019) Rotating-drum solar still with enhanced evaporation and condensation techniques: comprehensive study. Energy Convers Manag 199:112024. https://doi.org/10.1016/j.enconman.2019.112024

Al-Fulaij HF (2011) Dynamic modelling of MSF (multi stage flash) desalination plant. Thesis. Department of Chemical Engineering, University College London, p 334

Alsaedi MK (2018) Atmospheric water harvesting by an anhydrate salt and its release by a photothermal process towards sustainable potable water production in arid regions, thesis. KAUST Res Repos. https://doi.org/10.25781/KAUST-I3517

Amrut Pawar A, Karthic A, Lee S, Pandit S, Jung SP (2020) Microbial electrolysis cells for electromethanogenesis: materials, configurations and operations. Environ Eng Res 27(1):200484. https://doi.org/10.4491/EER.2020.484

Asiabanpour B, Ownby N, Summers M, Moghimi F (2019) Atmospheric water generation and energy consumption: an empirical analysis. In: 2019 IEEE Texas power and energy conference TPEC 2019, pp 1–6. https://doi.org/10.1109/TPEC.2019.8662164

Aye L, George B, Wu D (2013) Solar chilled drinking water sourced from thin air: modelling and simulation of a solar powered atmospheric water generator. In: Adapting to change: the multiple roles of modelling. pp 50–6

Bautista-Olivas AL, Cruz-Bautista F, Álvarez-Chávez CR, Zavala-Reyna AG, Sánchez-Landero LA, Alvarado-Ibarra J et al (2017) Concentration of heavy metals in condensed atmospheric water vapor at three Mexican localities. Atmósfera 30:209–220. https://doi.org/10.20937/ATM.2017.30.03.02

Bergmair D, Metz SJ, De van Lange HC, Steenhoven AA (2014) System analysis of membrane facilitated water generation from air humidity. Desalination 339:26–33. https://doi.org/10.1016/J.DESAL.2014.02.007

Beysens D, Milimouk I (2000) The case for alternative fresh water sources. Environ Sci 11:1–16

Bradshaw AJ (2016) Water harvesting methods and the built environment: The role of water harvesting methods and the built environment: the role of architecture in providing water security. MSc thesis. UNLV M. Arch. https://doi.org/10.34917/9112039

Chen B, Wang M, Tu Z, Gong X, Zhang H, Pan M et al (2015) Moisture dehumidification and its application to a 3kW proton exchange membrane fuel cell stack. Int J Hydrog Energy 40:1137–1144. https://doi.org/10.1016/j.ijhydene.2014.11.076

Dash A, Mohapatra A, Dash A (2015) (ATMOSPHERIC WATER GENERATOR) AWG: to meet the drinking water requirements of a household in coastal regions of India (MSc. thesis). Department of Mechanical Engineering, NIT, Rourkela, Odisha.

Ejeian M, Entezari A, Wang RZ (2020) Solar powered atmospheric water harvesting with enhanced LiCl /$MgSO_4$/ACF composite. Appl Therm Eng 176:115396. https://doi.org/10.1016/j.applthermaleng.2020.115396

El-Dessouky H, Ettouney H (2002) Fundamentals of salt water desalination. Elsevier B.V, Amsterdam (**ISSN: 978-0-444-50810-2**)

El-Hasan TS (2017) (Enhanced atmospheric moisture scavenging apparatus) EAMSA powered by (photovoltaic) PV solar system. Int Multidiscip Sci GeoConf Surv Geol Min Ecol Manag SGEM 17:659–666. https://doi.org/10.5593/sgem2017H/43/S29.083

Elashmawy M (2017) An experimental investigation of a parabolic concentrator solar tracking system integrated with a tubular solar still. Desalination 411:1–8. https://doi.org/10.1016/j.desal.2017.02.003

Elashmawy M (2020a) Experimental study on water extraction from atmospheric air using tubular solar still. J Clean Prod. https://doi.org/10.1016/j.jclepro.2019.119322

Elashmawy M (2020b) Improving the performance of a PCST-TSS (parabolic concentrator solar tracking-tubular solar still) using gravel as a sensible heat storage material. Desalination 473:114182. https://doi.org/10.1016/j.desal.2019.114182

Elashmawy M (2020) Alatawi I (2020) Atmospheric water harvesting from low-humid regions of hail city in Saudi Arabia. Nat Resour Res 29:3689–3700. https://doi.org/10.1007/S11053-020-09662-Y

Entezari A, Ejeian M, Wang R (2020) Super atmospheric water harvesting hydrogel with alginate chains modified with binary salts. ACS Mater Lett 2:471–477. https://doi.org/10.1021/acsmaterialslett.9b00315

Essa FA, Elsheikh AH, Sathyamurthy R, Muthu Manokar A, Kandeal AW, Shanmugan S et al (2020) Extracting water content from the ambient air in a double-slope half-cylindrical basin solar still using silica gel under Egyptian conditions. Sustain Energy Technol Assess 39:100712. https://doi.org/10.1016/j.seta.2020.100712

Garrido J, Casanovas A (2014) The central role of the Peltier coefficient in thermoelectric cooling. J Appl Phys 115:123517. https://doi.org/10.1063/1.4869776

Gido B, Friedler E, Broday DM (2016) Assessment of atmospheric moisture harvesting by direct cooling. Atmos Res 182:156–162. https://doi.org/10.1016/j.atmosres.2016.07.029

Gleick P (1993) Water in crisis: a guide to the world's fresh water resources. Oxford University Press, New York

Gomez WRG (2019) Design and development of an integrated automation simulation system. Int J Integr Eng 11(8):41–54

Guo R, Jiao T, Li R, Chen Y, Guo W, Zhang L, Zhou J, Zhang Q, Peng Q (2018) Sandwiched Fe_3O_4/carboxylate graphene oxide nanostructures constructed by layer-by-layer assembly for highly efficient and magnetically recyclable dye removal. ACS Sustain Chem Eng 6(1):1279–1288. https://doi.org/10.1021/acssuschemeng.7b03635

Gupta S (2018) Low temperature desiccants in atmospheric water generation. Electronic Theses and Dissertations. https://doi.org/10.18297/etd/3087

He W, Yu P, Hu Z, Lv S, Qin M, Yu C (2019) Experimental study and performance analysis of a portable (atmospheric water generator) AWG. Energies 13:1–1

Henninger SK, Ernst SJ, Gordeeva L, Bendix P, Fröhlich D, Grekova AD et al (2017) New materials for adsorption heat transformation and storage. Renew Energy 110:59–68. https://doi.org/10.1016/J.RENENE.2016.08.041

Herman H, Grobbelaar SS, Pistorius C (2020) The design and development of technology platforms in a developing country healthcare context from an ecosystem perspective. BMC Med Inform Decis Mak 20:1–24. https://doi.org/10.1186/S12911-020-1028-0

Huajun W, Chengying Q (2010) Study of operation performance of a low power thermoelectric cooling dehumidifier. Int J Energy Environ Exp 1:459–466

Inbar O, Gozlan I, Ratner S, Aviv Y, Sirota R, Avisar D (2020) Producing safe drinking water using an (atmospheric water

generator) AWG in an urban environment. Water (switzerland) 12:1–19. https://doi.org/10.3390/w12102940
Jiao T, Zhao H, Zhou J, Zhang Q, Luo X, Hu J, Peng Q, Yan X (2015) Activating hematite nanoplates via partial reduction for electrocatalytic oxygen reduction reaction. ACS Sustain Chm Eng 3(12):3130–3139. https://doi.org/10.1021/acssuschemeng.5b00695
Jung SP, Kim E, Koo B (2018) Effects of wire-type and mesh-type anode current collectors on performance and electrochemistry of microbial fuel cells. Chemosphere 209:542–550. https://doi.org/10.1016/j.chemosphere.2018.06.070
Jury WA, Vaux HJ (2007) The emerging global water crisis: managing scarcity and conflict between water users. Adv Agron 95:1–76. https://doi.org/10.1016/S0065-2113(07)95001-4
Kabeel AE (2006) Application of sandy bed solar collector system for water extraction from air. Int J Energy Res 30:381–394. https://doi.org/10.1002/er.1155
Kabeel AE, Omara ZM, Essa FA (2014) Enhancement of modified solar still integrated with external condenser using nanofluids: an experimental approach. Energy Convers Manag 78:493–498. https://doi.org/10.1016/j.enconman.2013.11.013
Kabeel AE, Abdulaziz M, El-Said EMS (2016) Solar-based atmospheric water generator utilization of a fresh water recovery: a numerical study. Int J Ambient Energy 37:68–75. https://doi.org/10.1080/01430750.2014.882864
Kabeel AE, Omara ZM, Essa FA (2017) Numerical investigation of modified solar still using nanofluids and external condenser. J Taiwan Inst Chem Eng 75:77–86. https://doi.org/10.1016/j.jtice.2017.01.017
Kadhim TJ, Abbas AK, Kadhim HJ (2020) Experimental study of atmospheric water collection powered by solar energy using the Peltier effect. IOP Conf Ser Mater Sci Eng. https://doi.org/10.1088/1757-899X/671/1/012155
Kang H, Kim E, Jung SP (2017a) Influence of flowrates to a reverse electro-dialysis (RED) stack on performance and electrochemistry of a microbial reverse electrodialysis cell (MRC). Int J Hydrog Energy. https://doi.org/10.1016/j.ijhydene.2017.06.187
Kang H, Jeong J, Gupta PL, Jung SP (2017b) Effects of brush-anode configurations on performance and electrochemistry of microbial fuel cells. Int J Hydrog Energy 42:27693–27700. https://doi.org/10.1016/j.ijhydene.2017.06.181
Khaligh A, Li Z (2010) Battery, ultra capacitor, fuel cell, and hybrid energy storage systems for electric, hybrid electric, fuel cell, and plug-in hybrid electric vehicles: state of the art. IEEE Trans Veh Technol 59:2806–2814. https://doi.org/10.1109/TVT.2010.2047877
Khalil B, Adamowski J, Shabbir A, Jang C, Rojas M, Reilly K et al (2016) A review: dew water collection from radiative passive collectors to recent developments of active collectors. Sustain Water Resou Manag 2:71–86. https://doi.org/10.1007/s40899-015-0038-z
Kim H, Rao SR, Kapustin EA, Zhao L, Yang S, Yaghi OM et al (2018) Adsorption-based atmospheric water harvesting device for arid climates. Nat Commun 9:1–8. https://doi.org/10.1038/s41467-018-03162-7
Koo B, Jung SP (2021) Improvement of air cathode performance in microbial fuel cells by using catalysts made by binding metal-organic framework and activated carbon through ultrasonication and solution precipitation. Chem Eng J 424:130388. https://doi.org/10.1016/J.CEJ.2021.130388
Koo B, Lee SM, Oh SE, Kim EJ, Hwang Y, Seo D, Kim JY, Kahng YH, Lee YW, Chung SY, Kim SJ, Park JH, Jung SP (2019) Addition of reduced graphene oxide to an activated-carbon cathode increases electrical power generation of a microbial fuel cell by enhancing cathodic performance. Electrochim Acta 297:613–622. https://doi.org/10.1016/j.electacta.2018.12.024
Kord SMZ (2019) Reviewing and designing atmospheric water generator. MSc thesis. Aalto University, Espoo, Finland. https://aaltodoc.aalto.fi/handle/123456789/41429. Accessed 23 Jan 2021
Kumar GRK, Sukumar SJ (2019) Solar powered atmospheric water generator. J Energy Environ Carbon Credits 9(2):8–10
Kumar PN, Manokar AM, Madhu B, Kabeel AE, Arunkumar T, Panchal H et al (2017) Experimental investigation on the effect of water mass in triangular pyramid solar still integrated to incline solar still. Groundw Sustain Dev 5:229–234. https://doi.org/10.1016/j.gsd.2017.08.003
Kumar V, Nandy A, Saha S, Ganguly S, Chattopadhyay S (n.d) A project on (atmospheric water generator) AWG with the concept of peltier effect. Int J Adva Comput Res, pp 2277–7970.
Kwan TH, Shen Y, Hu T, Pei G (2020a) Passively improving liquid sorbent based atmospheric water generation by integration of fuel cell waste products. J Clean Prod. https://doi.org/10.1016/j.jclepro.2020.125007
Kwan TH, Shen Y, Hu T, Pei G (2020b) The fuel cell and atmospheric water generator hybrid system for supplying grid-independent power and freshwater. Appl Energy 279:115780. https://doi.org/10.1016/j.apenergy.2020.115780
LaPotin A, Zhong Y, Zhang L, Zhao L, Leroy A, Kim H et al (2021) Dual-stage atmospheric water harvesting device for scalable solar-driven water production. Joule 5:166–182. https://doi.org/10.1016/J.JOULE.2020.09.008
Lee HS (2010) Thermal design: heat sinks, thermoelectrics, heat pipes, compact heat exchangers, and solar cells. Wiley Press, Hoboken. https://doi.org/10.1002/9780470949979
Li R, Shi Y, Alsaedi M, Wu M, Shi L, Wang P (2018) Hybrid hydrogel wit high water vapor harvesting capacity for deployable solar-driven atmospheric water generator. Environ Sci Technol 52:11367–11377. https://doi.org/10.1021/acs.est.8b02852
Liso V, Simon Araya S, Olesen AC, Nielsen MP, Kær SK (2016) Modeling and experimental validation of water mass balance in a PEM fuel cell stack. Int J Hydrog Energy 41:3079–3092. https://doi.org/10.1016/j.ijhydene.2015.10.095
Liu S, He W, Hu D, Lv S, Chen D, Wu X et al (2017) Experimental analysis of a portable atmospheric water generator by thermoelectric cooling method. Energy Procedia 142:1609–1614. https://doi.org/10.1016/J.EGYPRO.2017.12.538
Mane S, Kadam P, Lahoti G, Kazi F, Singh NM (2016) Optimal load balancing strategy for hybrid energy management system in DC (direct current) micro grid with PV, fuel cell and battery storage. In: 2016 IEEE international conference on renewable energy research and application ICRERA 2016 vol 5. pp 851–6. https://doi.org/10.1109/ICRERA.2016.7884456
Martinez E (2020) Härvist AWG (Atmospheric water generator) system for the Ag hub sustainability center. MSc thesis 2020, Master of Science in Industrial Design, G. D. Hines College of Architecture & Design, University of Houston

Mekhilef S, Saidur R, Safari A (2012) Comparative study of different fuel cell technologies. Renew Sustain Energy Rev 16:981–989. https://doi.org/10.1016/j.rser.2011.09.020

Mendoza-Escamilla JA, Hernandez-Rangel FJ, Cruz-Alcántar P, Saavedra-Leos MZ, Morales-Morales J, Figueroa-Diaz RA et al (2019) A feasibility study on the use of an (atmospheric water generator) AWG for the harvesting of fresh water in a semi-arid region affected by mining pollution. Appl Sci. https://doi.org/10.3390/app9163278

Milani D, Qadir A, Vassallo A, Chiesa M, Abbas A (2014) Experimentally validated model for atmospheric water generation using a solar assisted desiccant dehumidification system. Energy Build 77:236–246. https://doi.org/10.1016/j.enbuild.2014.03.041

Mittal H, Al Alili A, Alhassan SM (2020) Adsorption isotherm and kinetics of water vapors on novel superporous hydrogel composites. Microporous Mesoporous Mater 299:110106. https://doi.org/10.1016/j.micromeso.2020.110106

Modi KV, Nayi KH, Sharma SS (2020) Influence of water mass on the performance of spherical basin solar still integrated with parabolic reflector. Groundw Sustain Dev 10:100299. https://doi.org/10.1016/j.gsd.2019.100299

Mulchandani A, Malinda S, Edberg J, Westerhoff P (2020) Sunlight-driven atmospheric water capture capacity is enhanced by nano-enabled photothermal desiccants. Environ Sci Nano 7:2584–2594. https://doi.org/10.1039/d0en00463d

Nam T, Kang H, Pandit S, Kim SH, Yoon S, Bae S, Jung SP (2020) Effects of vertical and horizontal configurations of different numbers of brush anodes on performance and electrochemistry of microbial fuel cells. J Clean Prod 277:124125. https://doi.org/10.1016/j.jclepro.2020.124125

Namboorimadathil BS, Ramachandran AM, Venugopal AA, Mohamed AP, Asok A, Pillai S (2020) Clean water from air utilizing black TiO_2-based photothermal nanocomposite sheets. ACS Appl Nano Mater 3:6827–6835. https://doi.org/10.1021/acsanm.0c01207

(National Research Council) NRC (1999) Identifying future drinking water contaminants (2017). National Academies Press, Washington. https://doi.org/10.17226/9595

Nayi KH, Modi KV (2018) Pyramid solar still: a comprehensive review. Renewa Sustain Energy Rev 81:136–148. https://doi.org/10.1016/j.rser.2017.07.004

Nørskov JK, Bligaard T, Logadottir A, Bahn S, Hansen LB, Bollinger M et al (2002) Universality in heterogeneous catalysis. J Catal 209:275–278

Oki T, Kanae S (2006) Global hydrological cycles and world water resources. Science 313(80):1068–1072. https://doi.org/10.1126/science.1128845

Olivier J, De Rautenbach CJ (2002) The implementation of fog water collection systems in South Africa. Atmos Res 64:227–238. https://doi.org/10.1016/S0169-8095(02)00094-7

Omara ZM, Kabeel AE, Essa FA (2015) Effect of using nanofluids and providing vacuum on the yield of corrugated wick solar still. Energy Convers Manag 103:965–972. https://doi.org/10.1016/j.enconman.2015.07.035

Orta D, Mudgett PD, Ding L, Drybread M, Schultz JR, Sauer RL (1998) Analysis of water from the space shuttle and Mir space station by ion chromatography and capillary electrophoresis. J Chromatogr A 804:295–304. https://doi.org/10.1016/S0021-9673(97)01289-2

Panchal H, Sadasivuni KK, Israr M, Thakar N (2019) Various techniques to enhance distillate output of tubular solar still: a review. Groundw Sustain Dev 9:100268. https://doi.org/10.1016/j.gsd.2019.100268

Pandit S, Savla N, Sonawane JM, Sani AM, Gupta PK, Mathuriya AS, Rai AK, Jadhav DA, Jung SP, Prasad R (2021) Agricultural waste and wastewater as feedstock for bioelectricity generation using microbial fuel cells: Recent advances. Fermentation. https://doi.org/10.3390/fermentation7030169

Patel K, Patel JR, Mudgal A (2019) Potential of (Atmospheric Water Generator) AWG for Water Recovery in coastal regions of India. J Lib Ryerson CA n.d: 1–3

Patel J, Patel K, Mudgal A, Panchal H, Sadasivuni KK (2020) Experimental investigations of atmospheric water extraction device under different climatic conditions. Sustain Energy Technol Assess 38:100677. https://doi.org/10.1016/j.seta.2020.100677

Perry S, Perry RH, Green DW, Maloney JO (2000) Perry's chemical engineers' handbook, vol 38. ACS Publications, Washington. https://doi.org/10.5860/choice.38-0966

Pontious K, Weidner B, Guerin N, Dates A, Pierrakos O, Altaii K (2016) Design of an atmospheric water generator: Harvesting water out of thin air. In: 2016 IEEE systems and information engineering design conference (sieds'16). INSTITUTE of electrical and Electronics Engineers Inc., pp 6–11. https://doi.org/10.1109/SIEDS.2016.7489327

Qi H, Wei T, Zhao W, Zhu B, Liu G, Wang P et al (2019) An interfacial solar-driven atmospheric water generator based on a liquid sorbent with simultaneous adsorption–desorption. Adv Mater. https://doi.org/10.1002/adma.201903378

Rakesh BK, Shayan A, Mithun Sharma MN, Mohan M, Karthik V (2016) Study, analysis and fabrication of thermoelectric cooling system. Int J Sci Dev Res 1:332–338

Ramya M, Roopa M (2020) (Atmospheric Water generator) AWG using Peltier device. Int J Eng Res Technol 8:1–4

Rao YVC (2003) An introduction to thermodynamics, 2nd edn. Universities Press, Cambridge

Runze D, Qingfen M, Hui L, Gaoping W, Wei Y, Guangfu C et al (2020) Experimental investigations on a portable atmospheric water generator for maritime rescue. J Water Reuse Desalin 10:30–44. https://doi.org/10.2166/WRD.2020.048

Salehi AA, Ghannadi-Maragheh M, Torab-Mostaedi M, Torkaman R, Asadollahzadeh M (2020a) A review on the water-energy nexus for drinking water production from humid air. Renew Sustain Energy Rev 120:109627. https://doi.org/10.1016/j.rser.2019.109627

Salehi AA, Ghannadi-Maragheh M, Torab-Mostaedi M, Torkaman R, Asadollahzadeh M (2020b) Hydrogel materials as an emerging platform for desalination and the production of purified water. Sep Purif Rev. https://doi.org/10.1080/15422119.2020.1789659

Salek F, Moghaddam AN, Naserian MM (2018) Thermodynamic analysis and improvement of a novel solar driven atmospheric water generator. Energy Convers Manag 161:104–111. https://doi.org/10.1016/j.enconman.2018.01.066

Sami S (2020) Investigation of performance of solar powered water generator. Int J Sustain Energy Environ Res 9:1–16. https://doi.org/10.18488/journal.13.2020.91.1.16

Sanjana Y, Shilpa JP, Varun GN Vignesh A (2019) AWG (Atmospheric water generator) and segregation. Int J Sci Res Rev 07(03).

Shweta P, Nerlekar (2017) (Atmospheric water generator) AWG: air drops. Int J Adv Res Trends Eng Technol 4:8–12

Sleiti AK, Al-Khawaja H, Al-Khawaja H, Al-Ali M (2021) Harvesting water from air using adsorption material—prototype and experimental results. Sep Purif Technol 257:117921. https://doi.org/10.1016/J.SEPPUR.2020.117921

Son S, Koo B, Chai H, Tran HVH, Pandit S, Jung SP (2021) Comparison of hydrogen production and system performance in a microbial electrolysis cell containing cathodes made of non-platinum catalysts and binders. J Water Process Eng 40(November):101844. https://doi.org/10.1016/j.jwpe.2020.101844

Srivastava S, Yadav A (2018) Economic analysis of water production from atmospheric air using scheffler reflector. Appl Water Sci 91(9):1–10. https://doi.org/10.1007/S13201-018-0883-7

Sultan A (2004) Absorption/regeneration non-conventional system for water extraction from atmospheric air. Renew Energy 29:1515–1535. https://doi.org/10.1016/S0960-1481(03)00020-X

Suryaningsih S, Nurhilal O (2016) Optimal design of an (atmospheric water generator) AWG based on (thermo-electric cooler) TEC for drought in rural area. AIP Conf Proc. https://doi.org/10.1063/1.4941874

Suzuki M (1994) Activated carbon fiber: fundamentals and applications. Carbon N Y 32:577–586. https://doi.org/10.1016/0008-6223(94)90075-2

Tajeddini F, Eslami M, Etaati N (2018) Thermodynamic analysis and optimization of water harvesting from air using thermoelectric coolers. Energy Convers Manag 174:24–26

Tibaquirá JE, Hristovski KD, Westerhoff P, Posner JD (2011) Recovery and quality of water produced by commercial fuel cells. Int J Hydrog Energy 36:4022–4028. https://doi.org/10.1016/j.ijhydene.2010.12.072

Tran HVH, Kim E, Jung SP (2021) Anode biofilm maturation time, stable cell performance time, and time-course electrochemistry in a single-chamber microbial fuel cell with a brush-anode. J Ind Eng Chem. https://doi.org/10.1016/j.jiec.2021.11.001

Trinchieri M (2019) Development and optimization of an innovative solar atmospheric water generator (Msc. thesis). Politecnico di Torino, Corso di laurea magistrale in Ingegneria Energetica E Nucleare. http://webthesis.biblio.polito.it/id/eprint/10265

Tripathi A, Tushar S, Pal S, Lodh S, Tiwari S, Desai RS (2016) AWG (atmospheric water generator). Int J Enhanc Res Sci Technol Eng 5:2319–7463

Tu Y, Wang R, Zhang Y, Wang J (2018) Progress and expectation of atmospheric water harvesting. Joule 2:1452–1475. https://doi.org/10.1016/j.joule.2018.07.015

Wang B, Li Y, Li S (2015) Micro atmospheric water generator based on PDMS. J Mech Electr Eng 08. http://en.cnki.com.cn/Article_en/CJFDTotal-JDGC201508012.htm. Accessed 25 Jan 2021

Wang JY, Wang RZ, Wang LW (2016) Water vapor sorption performance of ACF-$CaCl_2$ and silica gel-$CaCl_2$ composite adsorbents. Appl Therm Eng 100:893–901. https://doi.org/10.1016/j.applthermaleng.2016.02.100

Wang JY, Liu JY, Wang RZ, Wang LW (2017) Experimental research of composite solid sorbents for fresh water production driven by solar energy. Appl Therm Eng 121:941–950. https://doi.org/10.1016/j.applthermaleng.2017.04.161

Wang X, Li X, Liu G, Li J, Hu X, Xu N et al (2019) An interfacial solar heating assisted liquid sorbent (Atmospheric Water Generator) AWG. Angew Chem (int Ed Engl) 58:12054–12058. https://doi.org/10.1002/anie.201905229

Wang M, Sun T, Wan D, Dai M, Ling S, Wang J et al (2021) Solar-powered nanostructured biopolymer hygroscopic aerogels for atmospheric water harvesting. Nano Energy 80:105569. https://doi.org/10.1016/j.nanoen.2020.105569

(World Energy Outlook) WEO (2016) Special report: water-energy Nexus—analysis—IEA n.d. https://www.iea.org/reports/water-energy-nexus. Accessed 22 Jan 2021

Xiao L, Shi R, Wu SY, Chen ZL (2019) Performance study on a (PHOTOVOLTAIC THERMAL) PV/T stepped solar still with a bottom channel. Desalination 471:114129. https://doi.org/10.1016/j.desal.2019.114129

Xing R, Wang W, Jiao T, Ma K, Zhang Q, Hong W, Qiu H, Zhou J, Zhang L, Peng Q (2017) Bioinspired polydopamine sheathed nanofibers containing carboxylate graphene oxide nanosheet for high-efficient dyes scavenger. ACS Sustain Chem Eng 5(6):4948–4956. https://doi.org/10.1021/acssuschemeng.7b00343

Xu Y, Wang R, Wang J, Li J, Jiao T, Liu Z (2021) Facile fabrication of molybdenum compounds (Mo_2C, MoP and MoS_2) nanoclusters supported on N-doped reduced graphene oxide for highly efficient hydrogen evolution reaction over broad pH range. Chem Eng J 417:129233. https://doi.org/10.1016/j.cej.2021.129233

Yang J, Zhang X, Qu H, Yu ZG, Zhang Y, Eey TJ et al (2020) A moisture-hungry copper complex harvesting air moisture for potable water and autonomous urban agriculture. Adv Mater. https://doi.org/10.1002/adma.202002936

Yuan Y, Zhang H, Yang F, Zhang N, Cao X (2016) Inorganic composite sorbents for water vapor sorption: a research progress. Renew Sustain Energy Rev 54:761–776. https://doi.org/10.1016/J.RSER.2015.10.069

Zahid M, Savla N, Pandit S, Thakur VK, Jung SP, Gupta PK, Prasad R, Marsili E (2022) Microbial desalination cell: desalination through conserving energy. Desalination 521:115381. https://doi.org/10.1016/J.DESAL.2021.115381

Zhang S, Chen B, Shu P, Luo M, Xie C, Quan S et al (2017) Evaluation of performance enhancement by condensing the anode moisture

in a proton exchange membrane fuel cell stack. Appl Therm Eng 120:115–120. https://doi.org/10.1016/j.applthermaleng.2017.03.128

Zheng X, Ge TS, Wang RZ, Hu LM (2014) Performance study of composite silica gels with different pore sizes and different impregnating hygroscopic salts. Chem Eng Sci 120:1–9. https://doi.org/10.1016/J.CES.2014.08.047